Profiling Human CMV-specific T cell responses reveals novel immunogenic ORFs

Rekha Dhanwani[1†], Sandeep Kumar Dhanda[1#], John Pham[1], Gregory P. Williams[1], John Sidney[1], Alba Grifoni[1], Gaelle Picarda[1,3], Cecilia S. Lindestam Arlehamn[1], Alessandro Sette[1,2,*], Chris A Benedict [1,3,*]

[1] Center for Infectious Disease and Vaccine Research, La Jolla Institute for Immunology, La Jolla, CA 92037, USA

[2] Department of Medicine, University of California San Diego, La Jolla, CA 92093, USA

[3]Center for Autoimmunity and Inflammation, La Jolla Institute for Immunology, La Jolla, CA 92037, USA

† Present Address: Division of Extramural Activities, National Institute of Allergy and Infectious Diseases, National Institute of Health, Rockville, MD 20852, USA

[#] Present Address: St. Jude Children's Research Hospital, Arlington, VA 22203

* Corresponding authors

Alessandro Sette

Email: alex@lji.org

Chris A. Benedict

Email: benedict@lji.org

Abstract

Despite the prevalence and medical significance of human cytomegalovirus (HCMV) infections, a systematic analysis of the targets of T cell recognition in humans that spans the entire genome and includes recently described potential novel ORFs is not available. Here, we screened a library of epitopes predicted to bind HLA class II that spans over 350 different HCMV ORFs and includes ~150 previously described and ~200 recently described potential novel ORFs using an ex vivo IFNγ fluorospot assay. We identified 235 unique HCMV specific epitopes derived from 100 ORFs, some previously described as immunodominant and others that were not previously described to be immunogenic. Of those, 41 belong to the set of recently reported novel ORFs, thus providing evidence that at least some of these are actually expressed *in vivo* in humans. These data reveal that the breadth of the human T cell response to HCMV is much greater than previously thought. The ORFs and epitopes identified will help elucidate how T cell immunity relates to HCMV pathogenesis and instruct ongoing HCMV vaccine research.

Importance

To understand the crucial role of adaptive immunity in controlling cytomegalovirus infection and disease, we systematically analyzed the CMV 'ORFeome' to identify new CMV epitopes targeted primarily by CD4 T cells in humans. Our study identified >200 new T cell epitopes derived from both canonical and novel ORFs, highlighting the substantial breadth of anti-CMV T cell response and providing new targets for vaccine design.

Introduction

Human cytomegalovirus (HCMV, HHV-5) is a β-herpesvirus that infects the majority of the world's population. Infection in healthy individuals is characterized by a primary asymptomatic phase followed by the establishment of lifelong persistence/latency in several cell types (1, 2). HCMV's 236 kbp double stranded DNA genome facilitates its persistence and reactivation when immunity is compromised, with both viral and cellular proteins controlling viral gene expression and regulating the dynamic and reversible latent-lytic cycle that develops over a lifelong infection (3, 4). Although largely persistent, its reactivation in immunocompromised populations, such as transplant recipients and AIDS patients, causes severe disease outcomes (5-11). Congenital infection in the developing fetus is also the leading infectious cause of birth defects (12-18). Moreover, the available antiviral drug therapies are insufficient and often toxic in young children (19-22). Consequently, HCMV is recognized as a major public health problem and development of a vaccine that prevents or at least mitigates virus-induced disease is a top priority (23-25) .

Although both humoral and cell mediated immune responses protect against HCMV infection, a considerable effort has been made towards identifying HCMV targets of CTL responses due to their pivotal role in controlling HCMV disease in immunocompromised individuals (26-29). However, HCMV targets of CD4+ T helper cells, which amplify CTL and antibody responses or may mediate direct antiviral activity themselves, remain to be explored in detail. In order to develop a successful HCMV vaccine, it is imperative to assess the large number of candidate viral proteins for their potential to induce robust CD4+ T cell responses.

Previous work from Sylwester et al. extensively characterized the canonical HCMV proteins that are targeted by CD4+ and CD8+ T cell responses (30), and work by many other groups have identified immunodominant epitopes derived from these that include the 65kDA phosphoprotein (UL83/pp65), immediate early protein 1 (UL123), tegument protein pp150 (UL32), envelope glycoprotein B (UL55), viral transcription factor IE2 (UL122), and major capsid protein (UL86) (31-38). However, a comprehensive analysis of HCMV epitope-specific T cell responses has been challenging, mainly due to the large size of virus and the evolving impact that persistent infection has on the memory pool. Stern-Ginossar et al. recently reported all the HCMV RNAs found to be associated with ribosomes in infected fibroblasts, increasing the potential number of ORFs the virus may encode by ~3 fold (39). Here, we designed a comprehensive screening approach to assess potential T cell responses against 563 of these ORFs, which included both previously reported and potentially novel HCMV proteins. 2593 15-mer peptides were predicted using computational algorithms, and a high throughput screen was performed using an IFNγ fluorospot assay to identify epitopes targeted by both CD8+ and CD4+ T cells in healthy HCMV-infected adults. This 'whole ORFeome' approach resulted in the identification of more than 200 new CD4+ and CD8+ T cell epitopes.

Results

Targets of HCMV T cell reactivity

To define the epitopes targeted by HCMV-specific T cell responses in healthy adults, we screened PBMCs of 19 subjects, 10 males and 9 females, recruited from the San Diego blood bank (SDBB). The HCMV seropositivity of all the subjects was confirmed by IgG ELISA **(Fig. S1A)**. We tested a total of 2593 15-mer HCMV peptides covering a total of 563 ORFs (39). Removing the predicted ORFs that were located entirely within longer ORFs resulted in a set of 359 completely unique ORFs. This set consists of approximately 150 “canonical” ORFs, with an additional 200 identified by ribosomal RNA profiling (39). These 15-mer peptides corresponded to epitopes likely to be dominant based on a bioinformatic method that predicts promiscuous binding to HLA class II molecules (40). Each ORF analyzed contained a minimum of 2 predicted epitopes, with the exception of very small ORFs of less than 15-20 amino acid residues, in which case at least one peptide was synthetized. The 2593 peptides were arranged in 89 pools of 28 to 30 15-mers. The PBMC reactivity of each of the 89 pools was assayed directly *ex vivo* using an IFN-γ Fluorospot assay. After identifying the pools that resulted in IFN-γ production in HCMV+ individuals, the top 10 most reactive pools (that, on average, accounted for more than 90% of the reactivity observed within each subject) were then deconvoluted to identify the specific epitopes (**Fig. S2)**. Representative results from the initial screening and the deconvolution of a pool in a representative subject are shown in **Fig. 1A-B.** In conclusion, the results shown here indicate that human T cell responses to HCMV recognize a wide breadth of different epitope specificities.

Characterization of CMV epitope-specific immune responses

The deconvolution of the top 10 pools from each subject identified widespread reactivity directed against 235 unique epitopes **(Fig. S3 and Table 1)**. Interestingly, females tended to show both a higher frequency and magnitude of epitope-specific responses when compared to males, although this did not reach statistical significance (**Fig. S4)**. On average, each subject recognized 25 epitopes (**Fig. 2A**) and all subjects recognized at least 2 (range 2-57, **Fig. 2B**). Specifically, 6 out of 19 donors recognized 21-30 epitopes**.** A quarter of the epitopes (58 of the 235 recognized) were recognized by three or more subjects **(Fig. 2C)**, and these accounted for 76% of the total T cell response **(Fig. 2D)**.

We further characterized the phenotype of the T cell responses directed against these 58 dominant epitopes by intracellular IFN-γ staining (representative results shown in **Fig. 3A**, with the flow cytometry gating strategy shown in **Fig. S5A**). In the majority of tested subjects, the responding T cells were CD4+. More specifically, 68% of all responding T cells were CD4+ and 13% contained both IFN-γ+ CD4+ and CD8+. In 18% of the cases, only CD8+ T cells responded to these 58 epitopes **(Fig. 3B)**. Similarly, if the magnitude of the response was considered, 70% of the IFN-γ response was attributable to CD4+ T cells and only 30% emanated from CD8+ T cells **(Fig. 3C)**. The fact that the responses were dominated by CD4+ T cells is consistent with the fact that the peptides tested were originally selected based on their predicted likelihood to bind HLA class II alleles. In turn, the occasional identification of epitope-specific CD8+ T cell responses in many cases likely reflects class I epitopes nested within the 15-mer epitopes tested in the

screen. Overall, these results indicate that, as expected, the screening strategy employed mostly identifies targets of CD4+ T cell reactivity.

Analysis of the ORF of origin of the identified epitopes

The 235 epitopes identified mapped to a total of 100 of the 359 unique ORFs screened. Of those, 28 ORFs contained >3 immunogenic peptides and 18 ORFs were recognized in 15% or more of the donors (**Fig. 4).** Notably, the previously well-characterized immunodominant ORFs such as envelope glycoprotein B (UL55), IE1 (UL123), tegument protein pp65 (UL83), major capsid protein UL86, IE2 (UL122), and pp150 (UL32) were amongst those associated with more than three immunogenic peptides**.**

To address the novelty of our findings, we compared our results with ORFs that have already been reported and curated in the Immune Epitope Database (IEDB http://www.iedb.org) (41), as a source of defined epitopes. Specifically, a query of the IEDB in October 2020 for previously characterized targets of T cell responses tested in at least 19 donors and with a minimum response frequency of 15% revealed 7 ORFs that match the conditions of our screening results: UL83/pp65 (ORFL205C), UL123/IE1 (ORFL264C), UL122/IE2 (ORFL265C), UL55/gB (ORFL145C), UL32/pp150 (ORFL92C), UL40 (ORFL105C) and UL98 (ORFL229W) **(Fig. 4)**.

The same query revealed three additional ORFs that were not identified in our screen. These ORFs were associated with a limited number of literature-reported and IEDB curated epitopes: UL75/gH (ORFL184C; 1 epitope), UL44/DNA-pol (ORFL112C.iORF1; 3 epitopes) and UL138 (ORFL313C; 1 epitope). Importantly, our

screen identified 93 ORFs that were not previously described as targets of T cell responses **(Fig. 5).**

Notably, 52 of these 93 ORFs were already described in the 'canonical HCMV' annotated genome, but not all have been described as targets of human T cell responses. Even more strikingly, 41 of these 93 ORFs corresponded to those viral mRNAs only identified by recent ribosomal profiling studies (39), providing evidence that they are translated in HCMV infected cells. These results indicate that our approach successfully re-identified known ORFs as targets of T cell responses, and perhaps most importantly, greatly expanded the repertoire of canonical and 'novel' ORFs recognized by T cells in healthy adults.

Novel identified epitope pools elicit antigen specific CD4+ T cell responses.

Lastly, we wanted to explore whether the epitopes identified in the presented study could, alone or in combination with previously described epitopes, be utilized to generate epitope "MegaPools'" (MP) (42-46) to allow detection of CMV-specific CD4 T cell responses. Accordingly, we generated a 'P235' MP encompassing the 235 CMV epitopes identified in the present study. As a comparison, we considered the commercially available CMV peptide pool (Mabtech, catalog 3619-1) encompassing a total of 42 CD4 and CD8 epitopes. Additionally, we synthetized a MP of known class II epitopes curated in the IEDB database, encompassing a total of 187 CD4 epitopes (IEDB-II, Table 2).

These MPs were tested with PBMC from a new cohort of 20 individuals (6 males and 14 females), which included both HCMV seropositive and seronegative donors (10 CMV^+ and 10 CMV^-, **Fig. S1B** for IgG ELISA CMV confirmation). None of the PBMC from these subjects were used in the original epitope mapping experiments. PBMCs were

177 stimulated with the Mabtech, P235, IEDB-II, or a combination of both P235/ IEDB-II MPs.
178 CD4+ T cell responses were measured as percentage of activation-induced marker assay
179 positive (OX40+ CD137+) CD4+ T cells and results are displayed in **Fig. 6** (flow cytometry
180 gating strategy shown in **Fig. S5B**).

181 All HCMV MPs tested were associated with significantly higher CD4 AIM
182 responses in HCMV+ individuals compared to HCMV- subjects as shown in **Fig. 5**
183 (statistical differences detailed in figure legend). When comparing AIM responses
184 between the HCMV pools, the P235, IEDB-II and P235/IEDB-II MPs were associated with
185 significantly higher HCMV-specific CD4 responses compared to the Mabtech pool
186 (geometric mean 0.15% vs 0.25% CD4 AIM+, p=0.01; and 0.15% vs 0.36%, p=0.004,
187 and 0.15% vs 0.46% CD4 AIM+, p=0.004, respectively by Wilcoxon test). This was
188 expected, as the Mabtech pool contains fewer epitopes which are also mainly CD8 T cell
189 specific. Additionally, the combination of the P235 and IEDB-II MPs elicited higher CD4
190 responses than either MP alone (geometric mean 0.25% vs 0.46% CD4 AIM+, p=0.0078
191 and 0.36% vs 0.46% CD4 AIM+, p=0.004, respectively by Wilcoxon test) and had the
192 highest magnitude response of all pools tested. This indicates that the combination of
193 known (IEDB-II MP) and novel epitopes and ORFs (P235 MP) can capture the broadest
194 range of CD4 T-cell responses in HCMV+ individuals, which has high potential for clinical
195 diagnostic use.
196
197
198

Discussion

In this study we have identified >200 new epitopes derived from 100 HCMV ORFs that induce virus-specific T cell responses. Importantly, this demonstrates that the current HLA peptide-binding prediction algorithms that we and others have refined over the last several decades are extremely efficient (47-51), and represent an excellent alternative to synthesizing genome-wide overlapping peptides, especially for large pathogens such as HCMV. Despite the significant diversity in the human HLA repertoire, current advances in algorithm-based epitope identification take into consideration epitopes with potential binding to diverse haplotypes, which undoubtedly contributed to this success (40, 52). Together, this approach allowed us to increase the known T cell epitope landscape for HCMV by greater than 10-fold by synthesizing only 2593 peptides, illustrating both its efficiency and cost effectiveness in deciphering immune targets of large pathogens.

We chose to use IFN-γ production as a readout for positive epitope reactivity in a fluorospot-based assay to identify HCMV-specific T cell epitopes in this study. As true for most viral infections, CMV drives a strong Th1-like CD4+ response, and most effector and memory viral CD8+ T cells also produce this cytokine (53). However, future studies assessing which of these 235 epitopes may elicit HCMV-specific CD4 T cells to produce other cytokines are merited. Previously, we have observed that Dengue virus epitope-specific CD4+ T cells can produce both IFNγ and IL-10 (54), something we have also seen during acute CMV infection in mice (55), where IL-10 producing CD4+ T cells enhance the duration of viral persistence (56). Recent studies by the Wills and Moss groups show that subsets of HCMV epitope-specific CD4+ T cells can produce IL-10 and also display cytolytic markers (57, 58). The potential CTL activity of HCMV-specific CD4+

T cells has been postulated for many years (59), and our recent results showing that CMV epitope-specific CD4 T cells can directly kill *in vivo* support this hypothesis (60). Taken together, our identification of >200 new T cell epitopes that elicit IFNγ production in this study provide us and others in the field valuable new tools to dissect the phenotypes and effector functions of HCMV-specific CD4 T cells in cases of both healthy and immune compromised patients, and will also help instruct ongoing vaccine efforts.

Of the 100 ORFs which we show here to be sources of specific T cell epitopes, 41 were uniquely identified as ribosome-bound RNAs in HCMV infected fibroblasts (39), with these 41 yielding 50 unique epitopes. Notably, of these 41 ORFs, 17 are predicted to produce proteins <50 amino acids in length, and 7 contain non-ATG start codons. This is consistent with recent studies suggesting that the short/'cryptic' mRNAs present in both virally infected and tumor cells can be translated, proteolytically processed and loaded onto HLA molecules, resulting in the induction of epitope-specific T cell responses (61-63). Interestingly, one of the larger 41 ORFs that contains two newly identified T cell epitopes (ORFL147C, 476 amino acids) has very recently been shown to regulate RNA binding/processing, and its deletion compromises CMV replication in fibroblasts (64). Despite >20% of the novel T cell epitopes identified here being derived from these newly described, ribosome-associated HCMV RNAs, no more than 2 of the 19 healthy donors analyzed produce T cells specific for any single one of these epitopes. This indicates that these novel ORFs 1) may not be broad targets of T cell responses in infected persons, 2) that specific individuals may more efficiently present epitopes derived from short/cryptic HCMV RNAs or 3) that minor HLA molecules may present them, with other possibilities also existing. Additionally, whether the proteins derived from these short ORFs are stable

and play a role in the HCMV lifecycle remains an open question. Finally, we also identified 24 epitopes derived from 14 'canonical' HCMV ORFs where the only historic support for their existence was the presence of their RNA in infected cells or bioinformatic analyses. Notably, a recent comprehensive study where 169 predicted canonical HCMV proteins (including these 14) were epitope-tagged, expressed stably in infected cells, immunoprecipitated and analyzed for interacting proteins by mass spectrometry supports our results that these ORFs are expressed as proteins (64).

Of the 59 canonical ORFs that we have identified here to contain T cell epitopes, >25% of these are known to function as immunomodulatory proteins (65). This is intriguing, as perhaps these HCMV proteins are more subject to being localized to antigen-processing or presentation compartments within infected cells. One of these epitopes is derived from the HCMV IL-10 orthologue, which is being considered as a potential HCMV vaccine candidate (66, 67). Additionally, 3 epitopes were found to be embedded within the viral UL128 protein, a critical component of the pentameric envelope protein complex (UL128-131/gH/gL) that mediates entry of HCMV into non-fibroblast cell types (68, 69). This is also of high potential interest in the context of vaccine development, as many believe the pentamer should be included in a viral- or subunit-based approach (70). Notably, both vIL-10 and UL128 have largely been considered only in the context of their abilities to induce antibody-based vaccine protection, but our identification of T cell epitopes derived from both these HCMV proteins suggests they may function to prime both humoral and cellular immunity.

Methods

Study design

For the initial CMV ORF screen, the responses of 19 CMV-seropositive subjects were evaluated. PBMCs were stimulated with 89 pools covering 563 ORFs of HCMV. Each pool comprised of 28-30 15-mer peptides overlapping by 10 residues. PBMCs that were found reactive to a pool were further tested against individual peptides contained in the pool using IFN-γ Fluorospot assay. Flow cytometry was then used to further characterize the epitopes recognized by PBMCs stimulated with individual peptides by detecting IFN-γ production from CD8+ and CD4+ T cells.

For the CMV-235 validation and comparison screen, the responses of a new cohort consisting of 10 CMV-seropositive and 10 seronegative subjects were evaluated. PBMCs were stimulated with CMV-Mabtech peptide pool (Catalog 3619-1), CMV-IEDB peptide pool (Table 2) (44, 46), CMV-235 pool, or a combination of both CMV-IEDB and CMV-235 pools. PBMC responses were assayed using the same IFN-γ Fluorospot assay. These studies were approved by the institutional review board committee at La Jolla Institute protocol number: VD-112 and VD-174.

Subjects

19 subjects (10 males and 9 females) were recruited anonymously from San Diego blood bank (SDBB) for the initial CMV ORF screens. For the CMV-235 comparison screens, samples from 20 subjects (6 males and 14 females) were obtained by La Jolla Institute Clinical Core and Continental Services Group (Miami, FL) for prior, unrelated studies. Blood samples were collected by trained staff. At the time of enrollment in the initial studies, all individual subjects provided informed consent that any leftover sample could be used for future studies, which includes this study. These subjects were

considered healthy as defined by no known history of any significant systemic diseases (not limited to autoimmune disease, diabetes, kidney or liver disease, congestive heart failure, malignancy, coagulopathy, hepatitis B or C, or HIV). The demographics of those subjects are provided in **Table 3**.

The IgG antibodies of the subjects for both cohorts were measured using Cytomegalovirus IgG Elisa kit from Genway Biotech Inc. according to manufacturer's instructions.

Peptide prediction

Based on the 7-allele method as previously described (40), 2593 peptides were predicted for 563 potential HCMV ORFs. Of the 751 ORFs predicted by ribosomal profiling (39), those smaller than 15 amino acids were excluded, and only one peptide of ORFs 15-20 amino acids in length were selected for screening.

Peptide libraries and pool preparation

The predicted peptides were commercially synthesized as crude material by TC Peptide Lab (www.tcpeptidelab.com; San Diego, CA). The peptides were solubilized in DMSO at a concentration of 20 mg/ml and spot checked for quality by mass spectrometry. The peptides were pooled into peptide pools containing 28-30 peptides constituting multiple ORFs per pool. A total of 89 pools were prepared covering 563 ORFs of HCMV. The final concentration of each pool was 0.7 mg/ml.

For the IEDB-II (Table 2) and P235 (Table 1) peptide pools peptides were synthesized by A&A ltd, San Diego, resuspended in DMSO, pooled and sequentially lyophilized as previously described (71). The IEDB-II peptide pool was developed based on data available in the IEDB (www.iedb.org) (41). The MHC class II restricted epitopes

for CMV was extracted from the IEDB in October of 2020 using the following query; Organism: human herpesvirus 5 (ID:10359), positive assays only, no B cell assays, MHC restriction type: class II, host: *Homo sapiens*. The resulting 187 epitopes (table 2) were filtered for size (13-20 amino acids) and discovered using one of the following assays: ELISPOT, ICS, multi- or tetramers, proliferation and "helper response". The CMV peptide pool for human CD4 and CD8 T cells containing 42 peptides (14 MHC class II restricted and 28 MHC class I restricted) representing pp50, pp65, IE1, IE2, and envelope glycoprotein B was purchased from Mabtech.

Isolation of PBMC by Ficoll-Paque density gradient centrifugation

One-unit blood from each donor was processed for PBMC isolation. Briefly, blood was centrifuged and the top layer of plasma was removed. The remaining blood was diluted and layered over 15 ml of Ficoll-Paque. Tubes were spun at room temperature in a swinging bucket rotor without brake applied. The PBMC interface was carefully removed by pipetting and washed with PBS by centrifugation at 800 rpm for 10 mins with brakes off. PBMC pellet was resuspended in RPMI media, cell number and viability were determined by trypan blue staining and cells were cryopreserved in liquid nitrogen in freezing media (90% Fetal bovine serum and 10% DMSO) at a density of 30 million/ml and stored until further processed.

Fluorospot assay

PBMC were thawed, washed and counted for viability using the trypan blue exclusion method. 200,000 cells were plated in triplicates and stimulated with pools (2µg/ml) or peptides (10µg/ml), PHA (10µg/ml) or medium containing equivalent amount of DMSO in 96- well plates (Immubilion-P, Millipore) previously coated with anti IFN-γ

antibody (1-D1K, Mabtech, Stockholm, Sweden). After 20 hr incubation at 37°C, cells were discarded and wells were washed six times with PBS/0.05% Tween 20 using an automated plate washer and further incubated with IFN-γ antibody (7-B6-1-FS-BAM) for 2 hrs at room temperature. After incubation, wells were washed and incubated with fluorophore conjugated anti-BAM-490 antibody for 1 hr at room temperature. Finally, the plates were washed and incubated with fluorescence enhancer for 15 min, blotted dry and fluorescent spots were counted by computer assisted image analysis (IRIS Fluorospot reader, Mabtech, Sweden).

Each pool or peptide was considered positive compared to the background that had equivalent amount of DMSO based on the following criteria: (i) 20 or more spot forming cells (SFC) per 10^6 PBMC after background subtraction, (ii) the stimulation index greater than 2, and (iii) $p<0.05$ by student's t test or Poisson distribution test when comparing the peptide or pool triplicates with the negative control triplicate.

Intracellular cytokine assay for IFN-γ

Intracellular staining for IFN-γ and flow cytometry was performed to detect antigen specific T cell responses. $1x10^6$ PBMCs suspended in RPMI medium supplemented with 1-% heat inactivated human AB serum, glutamine and penicillin streptomycin were plated in U-bottom 96 well plates. After overnight resting at 37°C, PBMCs were spun and replaced with fresh RPMI media and stimulated with individual peptides at a concentration of 10 µg/ml. PHA at a concentration of 5 µg/ml was used as a positive control. After 1 hr of incubation at 37°C, 2µg/ml of Brefeldin was added and cell were further incubated at 37°C for additional 5 hrs. The cells were then harvested, washed with 200 µl of MACS Buffer and stained with a cocktail of antibodies that contained CD3-Af700 (eBioscience,

clone UCHT1), CD4-APCef780 (eBioscience, clone RPA-T4), CD8-BV650 (Biolegend, clone RPA-T8), CD14-V500 (BD Biosciences, clone M5E2), CD19-V500 (BD Biosciences, clone HIB19), and fixable viability dye-e506 for 30 min at 4°C. The cells were then washed thrice with 200 µl MACS buffer, fixed using 4% PFA for 10 mins at 4°C, washed with 200 µl PBS and rested at 4°C overnight in 200 µl MACS buffer. The following day, cells were washed, permeabilized by washing with 200 µl saponin buffer (0.5 % saponin in PBS), washed with blocking buffer (10% human serum prepared in saponin buffer) and stained with IFN-γ-FITC (eBioscience, clone 4S.B3) antibody at room temperature for 30 mins. The cells were finally washed with PBS and suspended in 200 µl PBS.

The cells were acquired on ZE5 Biorad plate reader and further analysis was done on FlowJo software. Gates were applied on live single cells for CD3+, CD4+ and CD8+ T cell populations. The percentage of reactive CD4+ or CD8+ IFN-γ T cells were expressed as a percent of the total number of parent population analyzed. Reactive populations met the following 2 criteria: (i) well-defined cell population positive for both IFN-γ and CD4 or CD8 constituting at least 0.02% (post subtracting their corresponding DMSO controls) of the total number of CD4+ or CD8+ cells analyzed (ii) stimulation index greater than 2.

Activation induced marker (AIM) assay

PBMC were thawed, washed and counted for viability using the trypan blue exclusion method. 1 million cells per donor/condition were plated and cultured in the presence of the CMV specific pools (1µg/mL for P235 and IEDB-II, 2µg/mL for Mabtech pool), PHA (10µg/mL), or medium containing equivalent amount of DMSO in 96-well U-bottom plates. Cells were then harvested, washed with 200µl of MACS Buffer and stained

with a cocktail of antibodies that contained CD3-Af700 (eBioscience, clone UCHT1), CD4-BV605 (eBioscience , clone RPA-T4), CD8-PerCP-Cy5.5 (Biolegend, clone HIT8a), CD14-V500 (BD Biosciences, clone M5E2), CD19-V500 (BD Biosciences, clone HIB19), OX40-PE-Cy7 (Ber-ACT35), CD137-APC (4B4-1), and fixable viability dye-e506 for 30 min at 4°C. The cells were then washed thrice with 200 µl MACS buffer, fixed using 4% PFA for 10 mins at 4°C, and resuspended in 200 µl of PBS for acquisition.

Cells were acquired on a BD LSRFortessa and further analysis was done on FlowJo software. As previously described (44, 72), quantification of live, singlet antigen specific CD4 T cells was determined as a percentage of their OX40+CD137+ expression (AIM+). CMV specific AIM+ CD4 T cell signals were background subtracted with their corresponding negative control DMSO samples, with a minimal DMSO level set to 0.005%. The limit of detection (LOD) for the AIM+ assay was calculated by multiplying the upper confidence interval of the geometric mean of all DMSO samples by 2 (0.03).

Statistical analysis

Statistical analyses were performed using GraphPad Prism versions 8.1.1 and 8.4.3. Statistical details are provided with each figure.

Acknowledgement

We would also like to thank all donors that participated in the study. We also thank the La Jolla Institute for Immunology Clinical Studies Group and Flow Cytometry Core for all the invaluable help.

Author contribution

AS and CAB conceived the study. RD and GW performed the experiments and analyzed the data. SKD performed peptide prediction, JP processed blood samples, RD, GW, and GP conducted ELISA, JS helped with the quality check of synthesized peptides, AG designed the IEDB-II pool, CLA, AS, CAB directed the study, RD, AS, CAB wrote the manuscript taking input from other authors.

Funding

This work was supported by NIH Grants AI139749 and AI101423 to C.A.B, and NIH contracts 75N93019C00065 to A.S. and 75N93019C00067 to C.L.A.

Conflict of interest

The authors declare that they have no conflict of interest.

References

1. Collins-McMillen D, Buehler J, Peppenelli M, Goodrum F. 2018. Molecular Determinants and the Regulation of Human Cytomegalovirus Latency and Reactivation. Viruses 10.
2. Hargett D, Shenk TE. 2010. Experimental human cytomegalovirus latency in CD14+ monocytes. Proc Natl Acad Sci U S A 107:20039-44.
3. Chaturvedi S, Klein J, Vardi N, Bolovan-Fritts C, Wolf M, Du K, Mlera L, Calvert M, Moorman NJ, Goodrum F, Huang B, Weinberger LS. 2020. A molecular mechanism for probabilistic bet hedging and its role in viral latency. Proc Natl Acad Sci U S A 117:17240-17248.
4. Davison AJ, Dolan A, Akter P, Addison C, Dargan DJ, Alcendor DJ, McGeoch DJ, Hayward GS. 2003. The human cytomegalovirus genome revisited: comparison with the chimpanzee cytomegalovirus genome. J Gen Virol 84:17-28.
5. Mattes FM, Vargas A, Kopycinski J, Hainsworth EG, Sweny P, Nebbia G, Bazeos A, Lowdell M, Klenerman P, Phillips RE, Griffiths PD, Emery VC. 2008. Functional impairment of cytomegalovirus specific CD8 T cells predicts high-level replication after renal transplantation. Am J Transplant 8:990-9.
6. Walker S, Fazou C, Crough T, Holdsworth R, Kiely P, Veale M, Bell S, Gailbraith A, McNeil K, Jones S, Khanna R. 2007. Ex vivo monitoring of human cytomegalovirus-specific CD8+ T-cell responses using QuantiFERON-CMV. Transpl Infect Dis 9:165-70.
7. Clarke LM, Duerr A, Feldman J, Sierra MF, Daidone BJ, Landesman SH. 1996. Factors associated with cytomegalovirus infection among human immunodeficiency virus type 1-seronegative and -seropositive women from an urban minority community. J Infect Dis 173:77-82.
8. Doyle M, Atkins JT, Rivera-Matos IR. 1996. Congenital cytomegalovirus infection in infants infected with human immunodeficiency virus type 1. Pediatr Infect Dis J 15:1102-6.
9. Duryea EL, Sanchez PJ, Sheffield JS, Jackson GL, Wendel GD, McElwee BS, Boney LF, Mallory MM, Owen KE, Stehel EK. 2010. Maternal human immunodeficiency virus infection and congenital transmission of cytomegalovirus. Pediatr Infect Dis J 29:915-8.
10. Kovacs A, Schluchter M, Easley K, Demmler G, Shearer W, La Russa P, Pitt J, Cooper E, Goldfarb J, Hodes D, Kattan M, McIntosh K. 1999. Cytomegalovirus infection and HIV-1 disease progression in infants born to HIV-1-infected women. Pediatric Pulmonary and Cardiovascular Complications of Vertically Transmitted HIV Infection Study Group. N Engl J Med 341:77-84.
11. Schoenfisch AL, Dollard SC, Amin M, Gardner LI, Klein RS, Mayer K, Rompalo A, Sobel JD, Cannon MJ. 2011. Cytomegalovirus (CMV) shedding is highly correlated with markers of immunosuppression in CMV-seropositive women. J Med Microbiol 60:768-774.
12. Demmler-Harrison GJ. 2009. Congenital cytomegalovirus: Public health action towards awareness, prevention, and treatment. J Clin Virol 46 Suppl 4:S1-5.

13. Jeon J, Victor M, Adler SP, Arwady A, Demmler G, Fowler K, Goldfarb J, Keyserling H, Massoudi M, Richards K, Staras SA, Cannon MJ. 2006. Knowledge and awareness of congenital cytomegalovirus among women. Infect Dis Obstet Gynecol 2006:80383.
14. Fowler KB, Stagno S, Pass RF, Britt WJ, Boll TJ, Alford CA. 1992. The outcome of congenital cytomegalovirus infection in relation to maternal antibody status. N Engl J Med 326:663-7.
15. Ross SA, Fowler KB, Ashrith G, Stagno S, Britt WJ, Pass RF, Boppana SB. 2006. Hearing loss in children with congenital cytomegalovirus infection born to mothers with preexisting immunity. J Pediatr 148:332-6.
16. Fowler KB, Boppana SB. 2006. Congenital cytomegalovirus (CMV) infection and hearing deficit. J Clin Virol 35:226-31.
17. Ross SA, Boppana SB. 2005. Congenital cytomegalovirus infection: outcome and diagnosis. Semin Pediatr Infect Dis 16:44-9.
18. Britt WJ. 2018. Maternal Immunity and the Natural History of Congenital Human Cytomegalovirus Infection. Viruses 10.
19. Griffiths PD. 2002. Strategies to prevent CMV infection in the neonate. Semin Neonatol 7:293-9.
20. Kimberlin DW, Lin CY, Sanchez PJ, Demmler GJ, Dankner W, Shelton M, Jacobs RF, Vaudry W, Pass RF, Kiell JM, Soong SJ, Whitley RJ, National Institute of A, Infectious Diseases Collaborative Antiviral Study G. 2003. Effect of ganciclovir therapy on hearing in symptomatic congenital cytomegalovirus disease involving the central nervous system: a randomized, controlled trial. J Pediatr 143:16-25.
21. Michaels MG, Greenberg DP, Sabo DL, Wald ER. 2003. Treatment of children with congenital cytomegalovirus infection with ganciclovir. Pediatr Infect Dis J 22:504-9.
22. Whitley RJ, Cloud G, Gruber W, Storch GA, Demmler GJ, Jacobs RF, Dankner W, Spector SA, Starr S, Pass RF, Stagno S, Britt WJ, Alford C, Jr., Soong S, Zhou XJ, Sherrill L, FitzGerald JM, Sommadossi JP. 1997. Ganciclovir treatment of symptomatic congenital cytomegalovirus infection: results of a phase II study. National Institute of Allergy and Infectious Diseases Collaborative Antiviral Study Group. J Infect Dis 175:1080-6.
23. Benedict CA. 2013. A CMV vaccine: TREATing despite the TRICKs. Expert Rev Vaccines 12:1235-7.
24. Permar SR, Schleiss MR, Plotkin SA. 2018. Advancing Our Understanding of Protective Maternal Immunity as a Guide for Development of Vaccines To Reduce Congenital Cytomegalovirus Infections. J Virol 92.
25. Plotkin SA, Boppana SB. 2019. Vaccination against the human cytomegalovirus. Vaccine 37:7437-7442.
26. Li CR, Greenberg PD, Gilbert MJ, Goodrich JM, Riddell SR. 1994. Recovery of HLA-restricted cytomegalovirus (CMV)-specific T-cell responses after allogeneic bone marrow transplant: correlation with CMV disease and effect of ganciclovir prophylaxis. Blood 83:1971-9.
27. Quinnan GV, Jr., Kirmani N, Rook AH, Manischewitz JF, Jackson L, Moreschi G, Santos GW, Saral R, Burns WH. 1982. Cytotoxic t cells in cytomegalovirus infection: HLA-restricted T-lymphocyte and non-T-lymphocyte cytotoxic responses correlate with recovery from cytomegalovirus infection in bone-marrow-transplant recipients. N Engl J Med 307:7-13.

28. Reusser P, Riddell SR, Meyers JD, Greenberg PD. 1991. Cytotoxic T-lymphocyte response to cytomegalovirus after human allogeneic bone marrow transplantation: pattern of recovery and correlation with cytomegalovirus infection and disease. Blood 78:1373-80.
29. Smith CJ, Quinn M, Snyder CM. 2016. CMV-Specific CD8 T Cell Differentiation and Localization: Implications for Adoptive Therapies. Front Immunol 7:352.
30. Sylwester AW, Mitchell BL, Edgar JB, Taormina C, Pelte C, Ruchti F, Sleath PR, Grabstein KH, Hosken NA, Kern F, Nelson JA, Picker LJ. 2005. Broadly targeted human cytomegalovirus-specific CD4+ and CD8+ T cells dominate the memory compartments of exposed subjects. J Exp Med 202:673-85.
31. Kern F, Bunde T, Faulhaber N, Kiecker F, Khatamzas E, Rudawski IM, Pruss A, Gratama JW, Volkmer-Engert R, Ewert R, Reinke P, Volk HD, Picker LJ. 2002. Cytomegalovirus (CMV) phosphoprotein 65 makes a large contribution to shaping the T cell repertoire in CMV-exposed individuals. J Infect Dis 185:1709-16.
32. Kern F, Surel IP, Faulhaber N, Frommel C, Schneider-Mergener J, Schonemann C, Reinke P, Volk HD. 1999. Target structures of the CD8(+)-T-cell response to human cytomegalovirus: the 72-kilodalton major immediate-early protein revisited. J Virol 73:8179-84.
33. Khan N, Best D, Bruton R, Nayak L, Rickinson AB, Moss PA. 2007. T cell recognition patterns of immunodominant cytomegalovirus antigens in primary and persistent infection. J Immunol 178:4455-65.
34. Khan N, Cobbold M, Keenan R, Moss PA. 2002. Comparative analysis of CD8+ T cell responses against human cytomegalovirus proteins pp65 and immediate early 1 shows similarities in precursor frequency, oligoclonality, and phenotype. J Infect Dis 185:1025-34.
35. Elkington R, Walker S, Crough T, Menzies M, Tellam J, Bharadwaj M, Khanna R. 2003. Ex vivo profiling of CD8+-T-cell responses to human cytomegalovirus reveals broad and multispecific reactivities in healthy virus carriers. J Virol 77:5226-40.
36. Elkington R, Shoukry NH, Walker S, Crough T, Fazou C, Kaur A, Walker CM, Khanna R. 2004. Cross-reactive recognition of human and primate cytomegalovirus sequences by human CD4 cytotoxic T lymphocytes specific for glycoprotein B and H. Eur J Immunol 34:3216-26.
37. Paston SJ, Dodi IA, Madrigal JA. 2004. Progress made towards the development of a CMV peptide vaccine. Hum Immunol 65:544-9.
38. Fuhrmann S, Streitz M, Reinke P, Volk HD, Kern F. 2008. T cell response to the cytomegalovirus major capsid protein (UL86) is dominated by helper cells with a large polyfunctional component and diverse epitope recognition. J Infect Dis 197:1455-8.
39. Stern-Ginossar N, Weisburd B, Michalski A, Le VT, Hein MY, Huang SX, Ma M, Shen B, Qian SB, Hengel H, Mann M, Ingolia NT, Weissman JS. 2012. Decoding human cytomegalovirus. Science 338:1088-93.
40. Paul S, Lindestam Arlehamn CS, Scriba TJ, Dillon MB, Oseroff C, Hinz D, McKinney DM, Carrasco Pro S, Sidney J, Peters B, Sette A. 2015. Development and validation of a broad scheme for prediction of HLA class II restricted T cell epitopes. J Immunol Methods 422:28-34.

41. Vita R, Mahajan S, Overton JA, Dhanda SK, Martini S, Cantrell JR, Wheeler DK, Sette A, Peters B. 2019. The Immune Epitope Database (IEDB): 2018 update. Nucleic Acids Res 47:D339-D343.
42. Bancroft T, Dillon MB, da Silva Antunes R, Paul S, Peters B, Crotty S, Lindestam Arlehamn CS, Sette A. 2016. Th1 versus Th2 T cell polarization by whole-cell and acellular childhood pertussis vaccines persists upon re-immunization in adolescence and adulthood. Cell Immunol 304-305:35-43.
43. da Silva Antunes R, Paul S, Sidney J, Weiskopf D, Dan JM, Phillips E, Mallal S, Crotty S, Sette A, Lindestam Arlehamn CS. 2017. Definition of Human Epitopes Recognized in Tetanus Toxoid and Development of an Assay Strategy to Detect Ex Vivo Tetanus CD4+ T Cell Responses. PLoS One 12:e0169086.
44. Grifoni A, Weiskopf D, Ramirez SI, Mateus J, Dan JM, Moderbacher CR, Rawlings SA, Sutherland A, Premkumar L, Jadi RS, Marrama D, de Silva AM, Frazier A, Carlin AF, Greenbaum JA, Peters B, Krammer F, Smith DM, Crotty S, Sette A. 2020. Targets of T Cell Responses to SARS-CoV-2 Coronavirus in Humans with COVID-19 Disease and Unexposed Individuals. Cell 181:1489-1501 e15.
45. Lindestam Arlehamn CS, McKinney DM, Carpenter C, Paul S, Rozot V, Makgotlho E, Gregg Y, van Rooyen M, Ernst JD, Hatherill M, Hanekom WA, Peters B, Scriba TJ, Sette A. 2016. A Quantitative Analysis of Complexity of Human Pathogen-Specific CD4 T Cell Responses in Healthy M. tuberculosis Infected South Africans. PLoS Pathog 12:e1005760.
46. Mateus J, Grifoni A, Tarke A, Sidney J, Ramirez SI, Dan JM, Burger ZC, Rawlings SA, Smith DM, Phillips E, Mallal S, Lammers M, Rubiro P, Quiambao L, Sutherland A, Yu ED, da Silva Antunes R, Greenbaum J, Frazier A, Markmann AJ, Premkumar L, de Silva A, Peters B, Crotty S, Sette A, Weiskopf D. 2020. Selective and cross-reactive SARS-CoV-2 T cell epitopes in unexposed humans. Science 370:89-94.
47. Nielsen M, Justesen S, Lund O, Lundegaard C, Buus S. 2010. NetMHCIIpan-2.0 - Improved pan-specific HLA-DR predictions using a novel concurrent alignment and weight optimization training procedure. Immunome Res 6:9.
48. Nielsen M, Lund O. 2009. NN-align. An artificial neural network-based alignment algorithm for MHC class II peptide binding prediction. BMC Bioinformatics 10:296.
49. Paul S, Kolla RV, Sidney J, Weiskopf D, Fleri W, Kim Y, Peters B, Sette A. 2013. Evaluating the immunogenicity of protein drugs by applying in vitro MHC binding data and the immune epitope database and analysis resource. Clin Dev Immunol 2013:467852.
50. Salimi N, Fleri W, Peters B, Sette A. 2012. The immune epitope database: a historical retrospective of the first decade. Immunology 137:117-23.
51. Wang P, Sidney J, Kim Y, Sette A, Lund O, Nielsen M, Peters B. 2010. Peptide binding predictions for HLA DR, DP and DQ molecules. BMC Bioinformatics 11:568.
52. Dhanda SK, Karosiene E, Edwards L, Grifoni A, Paul S, Andreatta M, Weiskopf D, Sidney J, Nielsen M, Peters B, Sette A. 2018. Predicting HLA CD4 Immunogenicity in Human Populations. Front Immunol 9:1369.
53. Lim EY, Jackson SE, Wills MR. 2020. The CD4+ T Cell Response to Human Cytomegalovirus in Healthy and Immunocompromised People. Front Cell Infect Microbiol 10:202.
54. Tian Y, Seumois G, De-Oliveira-Pinto LM, Mateus J, Herrera-de la Mata S, Kim C, Hinz D, Goonawardhana NDS, de Silva AD, Premawansa S, Premawansa G, Wijewickrama A,

Balmaseda A, Grifoni A, Vijayanand P, Harris E, Peters B, Sette A, Weiskopf D. 2019. Molecular Signatures of Dengue Virus-Specific IL-10/IFN-gamma Co-producing CD4 T Cells and Their Association with Dengue Disease. Cell Rep 29:4482-4495 e4.

55. Wehrens EJ, Wong KA, Gupta A, Khan A, Benedict CA, Zuniga EI. 2018. IL-27 regulates the number, function and cytotoxic program of antiviral CD4 T cells and promotes cytomegalovirus persistence. PLoS One 13:e0201249.

56. Humphreys IR, de Trez C, Kinkade A, Benedict CA, Croft M, Ware CF. 2007. Cytomegalovirus exploits IL-10-mediated immune regulation in the salivary glands. J Exp Med 204:1217-25.

57. Jackson SE, Sedikides GX, Mason GM, Okecha G, Wills MR. 2017. Human Cytomegalovirus (HCMV)-Specific CD4(+) T Cells Are Polyfunctional and Can Respond to HCMV-Infected Dendritic Cells In Vitro. J Virol 91.

58. Pachnio A, Ciaurriz M, Begum J, Lal N, Zuo J, Beggs A, Moss P. 2016. Cytomegalovirus Infection Leads to Development of High Frequencies of Cytotoxic Virus-Specific CD4+ T Cells Targeted to Vascular Endothelium. PLoS Pathog 12:e1005832.

59. van Leeuwen EM, Remmerswaal EB, Vossen MT, Rowshani AT, Wertheim-van Dillen PM, van Lier RA, ten Berge IJ. 2004. Emergence of a CD4+CD28- granzyme B+, cytomegalovirus-specific T cell subset after recovery of primary cytomegalovirus infection. J Immunol 173:1834-41.

60. Verma S, Weiskopf D, Gupta A, McDonald B, Peters B, Sette A, Benedict CA. 2016. Cytomegalovirus-Specific CD4 T Cells Are Cytolytic and Mediate Vaccine Protection. J Virol 90:650-8.

61. Erhard F, Dolken L, Schilling B, Schlosser A. 2020. Identification of the Cryptic HLA-I Immunopeptidome. Cancer Immunol Res 8:1018-1026.

62. Erhard F, Halenius A, Zimmermann C, L'Hernault A, Kowalewski DJ, Weekes MP, Stevanovic S, Zimmer R, Dolken L. 2018. Improved Ribo-seq enables identification of cryptic translation events. Nat Methods 15:363-366.

63. Laumont CM, Perreault C. 2018. Exploiting non-canonical translation to identify new targets for T cell-based cancer immunotherapy. Cell Mol Life Sci 75:607-621.

64. Nobre LV, Nightingale K, Ravenhill BJ, Antrobus R, Soday L, Nichols J, Davies JA, Seirafian S, Wang EC, Davison AJ, Wilkinson GW, Stanton RJ, Huttlin EL, Weekes MP. 2019. Human cytomegalovirus interactome analysis identifies degradation hubs, domain associations and viral protein functions. Elife 8.

65. Picarda G, Benedict CA. 2018. Cytomegalovirus: Shape-Shifting the Immune System. J Immunol 200:3881-3889.

66. Deere JD, Chang WLW, Villalobos A, Schmidt KA, Deshpande A, Castillo LD, Fike J, Walter MR, Barry PA, Hartigan-O'Connor DJ. 2019. Neutralization of rhesus cytomegalovirus IL-10 reduces horizontal transmission and alters long-term immunity. Proc Natl Acad Sci U S A 116:13036-13041.

67. Eberhardt MK, Deshpande A, Chang WL, Barthold SW, Walter MR, Barry PA. 2013. Vaccination against a virus-encoded cytokine significantly restricts viral challenge. J Virol 87:11323-31.

68. Nguyen CC, Kamil JP. 2018. Pathogen at the Gates: Human Cytomegalovirus Entry and Cell Tropism. Viruses 10.

69. Vanarsdall AL, Johnson DC. 2012. Human cytomegalovirus entry into cells. Curr Opin Virol 2:37-42.
70. Gerna G, Lilleri D. 2019. Human cytomegalovirus (HCMV) infection/re-infection: development of a protective HCMV vaccine. New Microbiol 42:1-20.
71. Carrasco Pro S, Sidney J, Paul S, Lindestam Arlehamn C, Weiskopf D, Peters B, Sette A. 2015. Automatic Generation of Validated Specific Epitope Sets. J Immunol Res 2015:763461.
72. Dan JM, Mateus J, Kato Y, Hastie KM, Yu ED, Faliti CE, Grifoni A, Ramirez SI, Haupt S, Frazier A, Nakao C, Rayaprolu V, Rawlings SA, Peters B, Krammer F, Simon V, Saphire EO, Smith DM, Weiskopf D, Sette A, Crotty S. 2021. Immunological memory to SARS-CoV-2 assessed for up to 8 months after infection. Science 371.

669 **Figures**

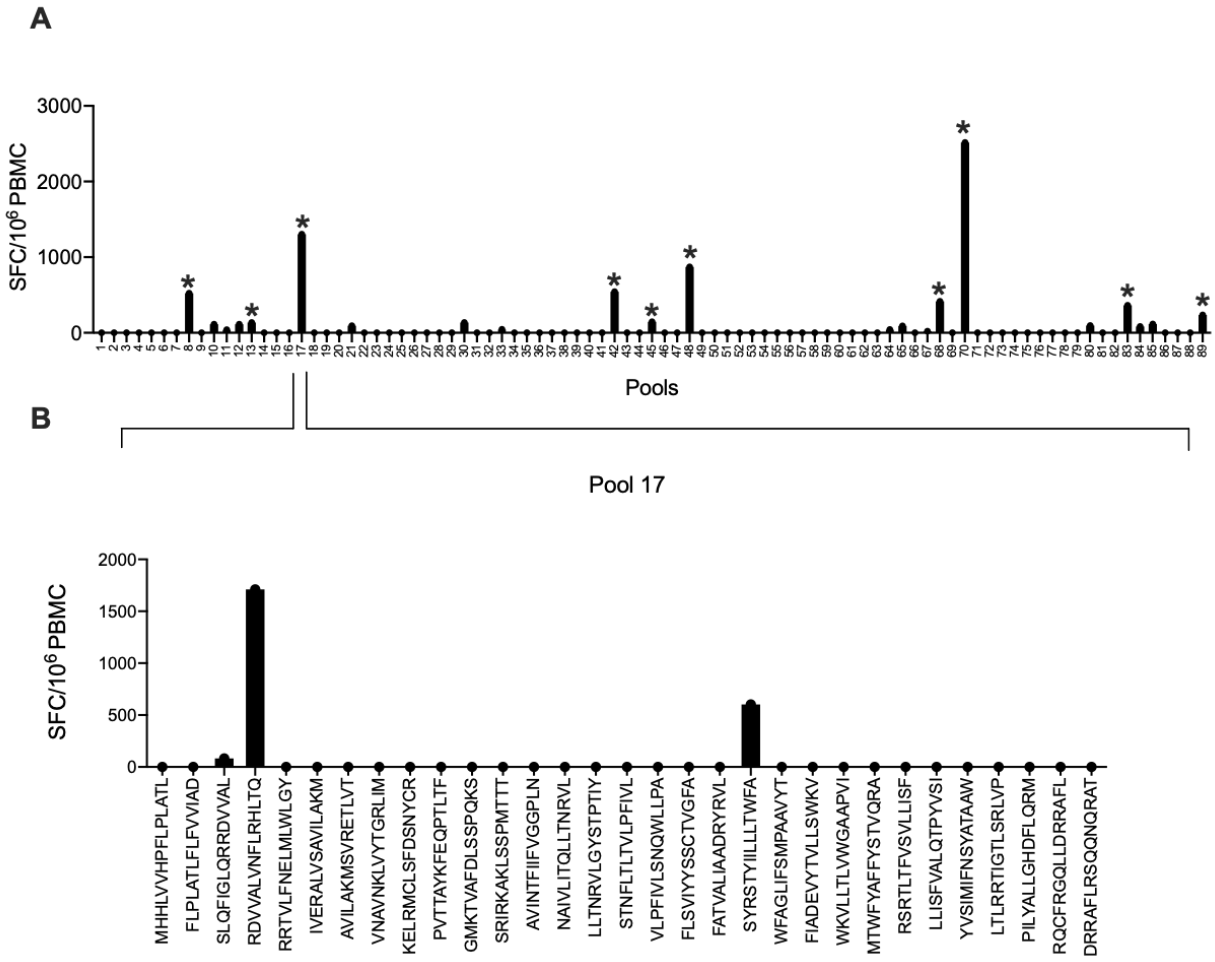

670

671 **Fig. 1 Strategy for HCMV epitope-specific T cell identification:** PBMCs from HCMV
672 seropositive subjects were stimulated with 2 µg/ml pools and plated on IFN-γ coated
673 fluorospot plates for 20 hours. The top 10 positive pools (indicated by * on bars) were
674 deconvoluted to identify individual epitopes. PBMC were stimulated with 10 µg/ml of each
675 individual peptide contained in the pool and reactivity was measured by IFN-γ fluorospot
676 assay. (A) SFC/10^6 PBMC for one representative subject against the 89 peptide pools (B)
677 Deconvoluted pool representing individual peptides.

678

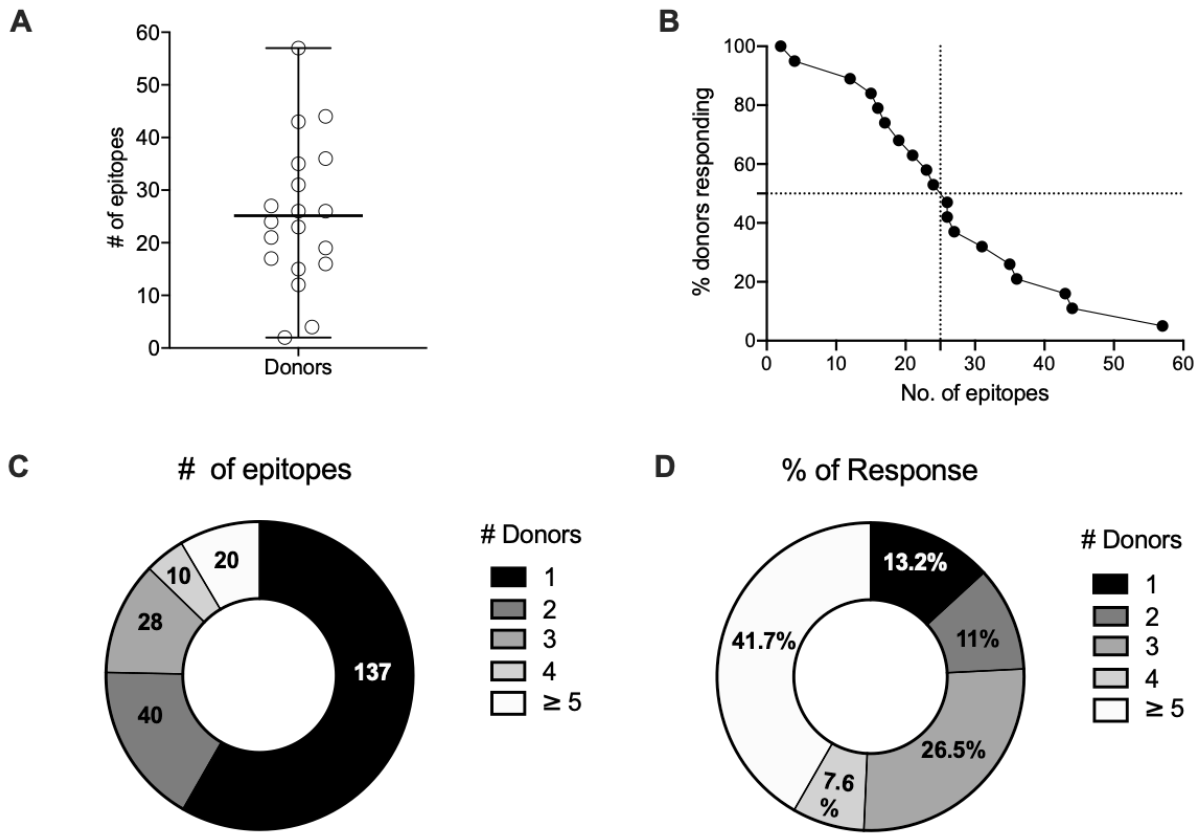

Fig. 2 Breadth and dominance of HCMV T cell responses: (A) The number of epitopes recognized by each donor, mean ± range. (B) Proportion of the 19 donors that responded to the indicated number of epitopes. (C) Epitopes by number of responding donors. (D) epitope % of total response by number of responding donors.

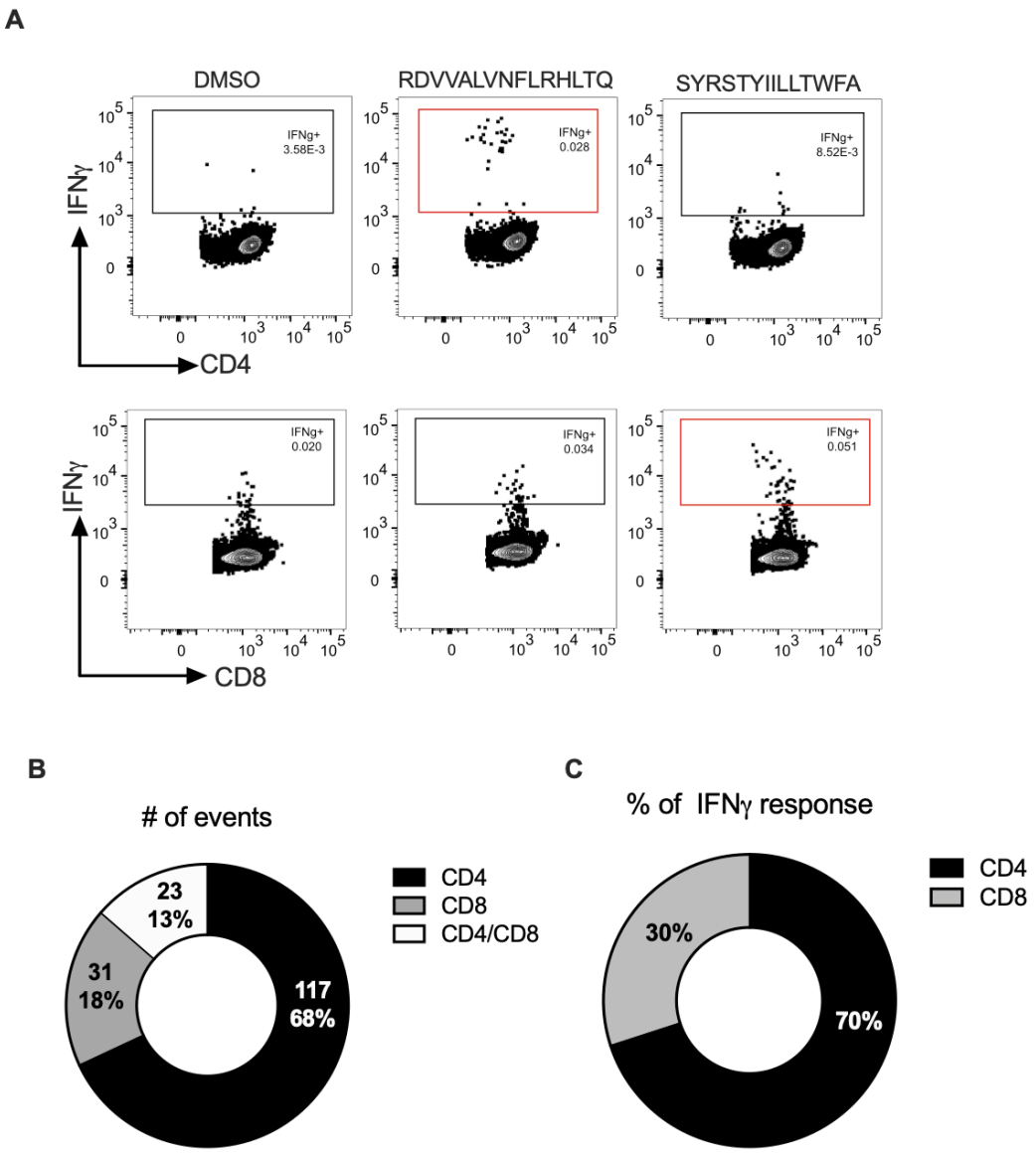

Fig. 3 Phenotypic characterization of HCMV T cell responses: (A) Representative FACS plots for intracellular IFN-γ production by CD4+ and CD8+ T cells (gating axis in red) upon stimulation with two of the scoring peptide epitopes that induced them (B and C). The number of events and % response attributable to CD4+ and CD8+ T cell responses of dominant epitopes (n=58) that demonstrated response frequency of 0.15 (15%) (i.e recognized by 3 or more donors).

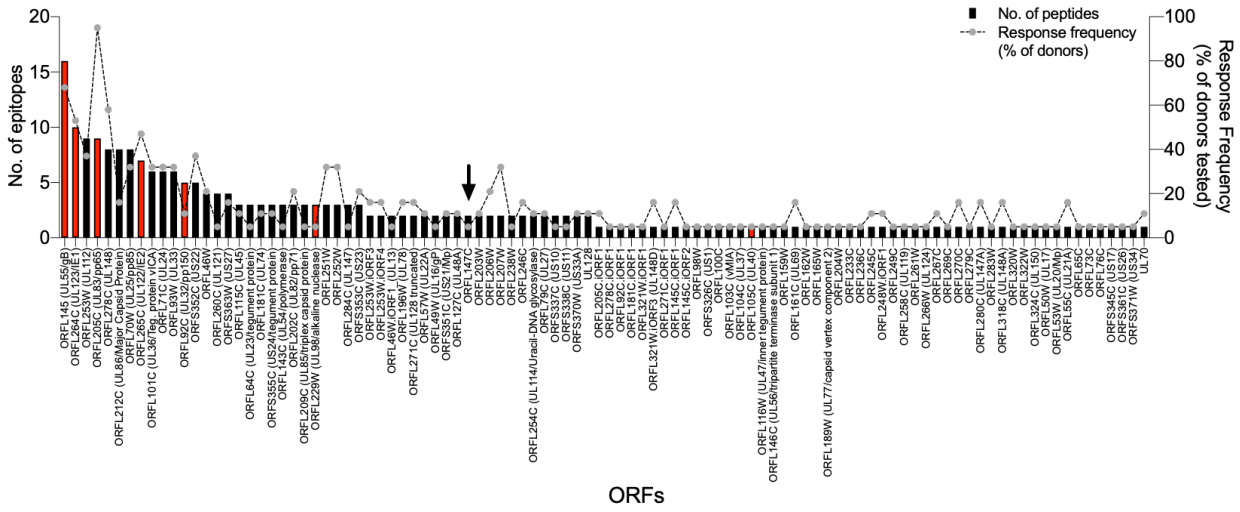

Fig. 4 T cell epitope distribution by ORF of origin: 235 epitopes mapped to 100 ORFs. Left Y axis denotes the number of epitopes associated with each ORF (bars) and right Y axis denotes the response frequency associated with each ORF (dotted line). Seven canonical ORFs that were common in IEDB and the present screen are denoted in red. ORFL147C (arrow) is the first 'novel' ORF identified by rRNA profiling from left-to-right, and only induces responses in 2/19 individuals tested.

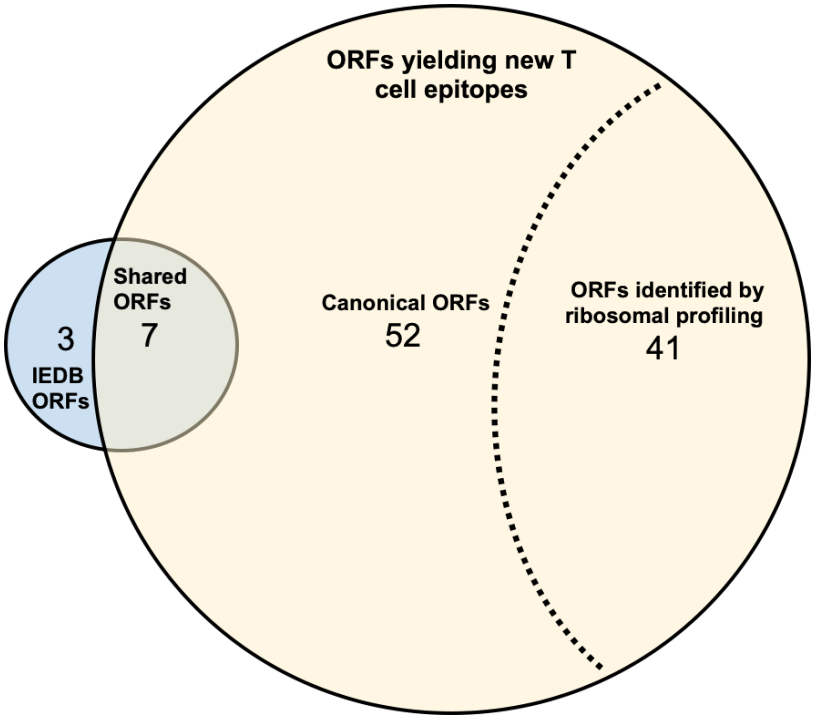

Fig. 5 Overlap between IEDB-reported and new immunogenic ORFs identified in this T cell epitope screen. New epitopes were identified in all 100 ORFS, including 7 ORFs previously reported in the IEDB to be targets of T cell responses. Of the 93 ORFs found to be new targets of T cells, 52 were canonical and 41 were 'novel' as identified by recent ribosomal mRNA profiling studies.

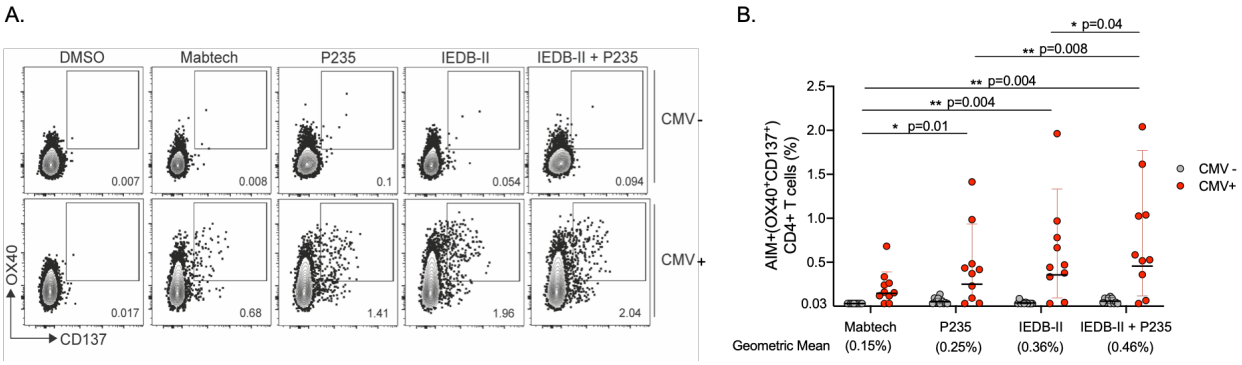

Fig. 6 Epitope specific CD4+ T cell responses in HCMV+ and HCMV- subjects detected with different peptide pools: (A) Representative FACS plots showing HCMV specific CD4+ T cell reactivity against different peptide pools based on activation-induced marker assays (OX40+ and CD137+ double expression). PBMCs from HCMV+ (red circles) and CMV- donors (grey circles) were stimulated with 2 µg/ml of the Mabtech pool or IEDB-II/P235 pools for 24 hrs. (B) Epitope-pool specific CD4+ T cells measured as percentage of activation-induced marker assay positive (OX40+ CD137+) CD4+ T cells. Each dot represents an individual subject. HCMV+ subjects demonstrated significantly higher CD4+ T cell AIM responses than HCMV- subjects with all the different pools tested. Mabtech HCMV+ vs HCMV- p=0.0007; P235 HCMV+ vs HCMV- p=0.0065; IEDB-II CMV+ vs CMV- p=0.0009; P235/IEDB-II CMV+ vs CMV- p=0.004. Two-tailed Mann-Whitney test. Comparisons across different pool formulations within the CMV+ were made using the Wilcoxon matched-pairs signed ranked test, Two-tailed p values are shown in the Figure; Geometric mean with geometric standard deviation.

Supplementary figures

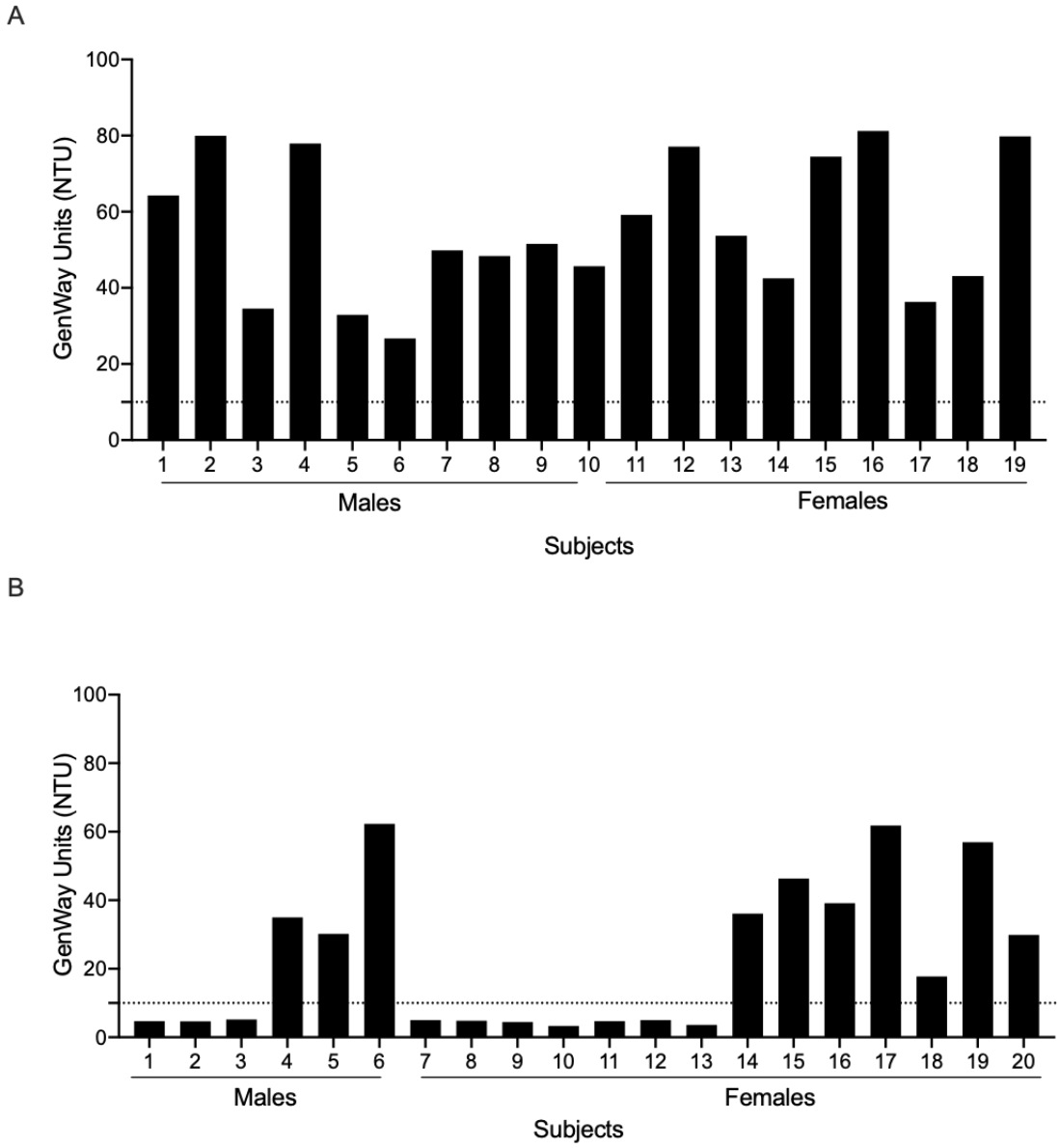

Fig. S1 Confirmation of HCMV seropositivity in donors. (A) IgG levels in plasma of subjects in the screening cohort (n=10 males, n=9 females) and (B) the validation cohort (n=13 males, n=26 females) determined by ELISA. Dotted line represents the cut off for positivity (10 NTU).

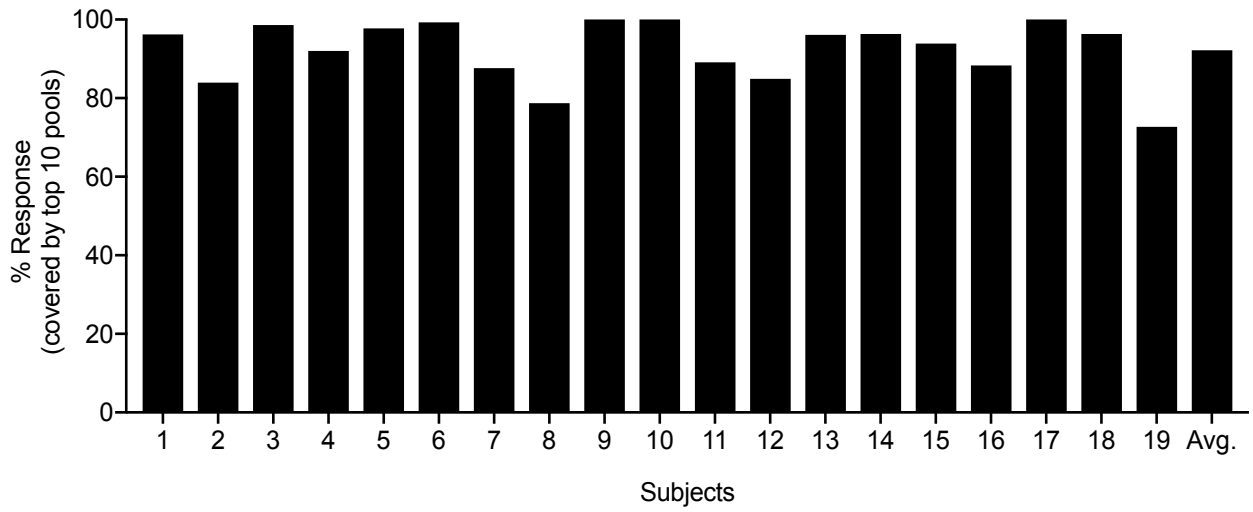

Fig. S2 The total T cell response captured by the top 10 epitope pools in each subject. The response magnitude of the top 10 pools as a percentage of the total response magnitude observed from all positive pools. On average, the top 10 pools accounted for ~90 % of each subject's total response.

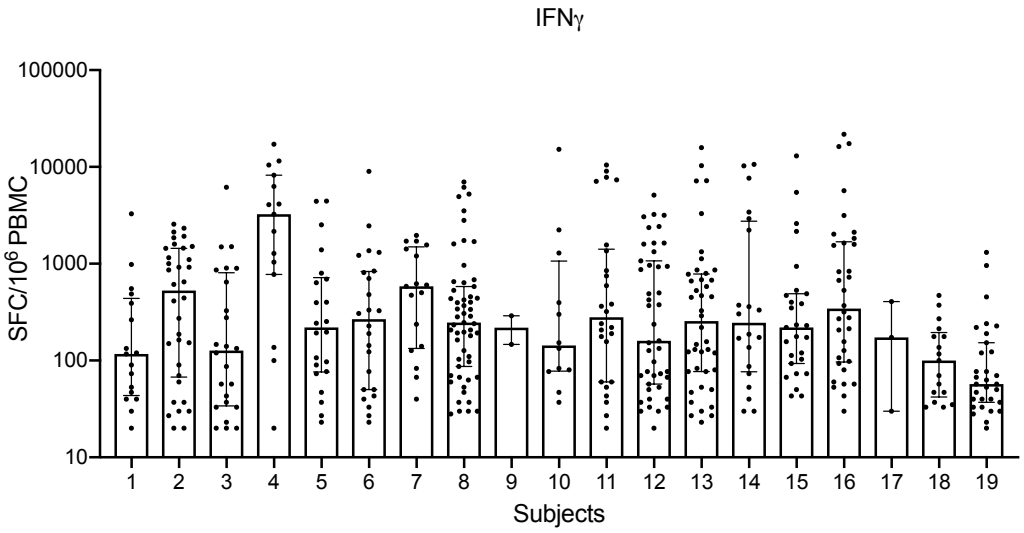

Fig. S3 Response magnitude of each epitope identified in HCMV seropositive individuals: Each dot represents an epitope. Y axis represents the response magnitude of individual epitopes. X axis represents each subject. Median ± interquartile range is shown.

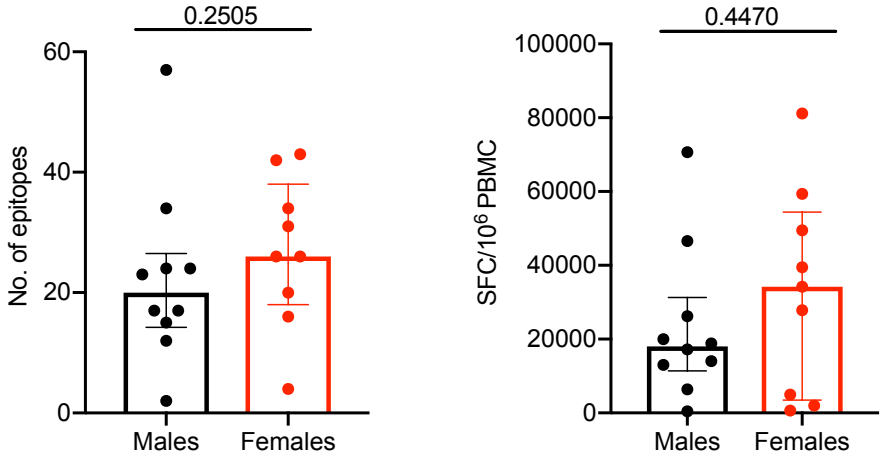

Fig. S4 Frequency and magnitude of response in males and females: Each dot represents a donor. Black dot/bar represents males and red dot/bar represents females. Median with interquartile range is displayed. Two-tailed Mann-Whitney test.

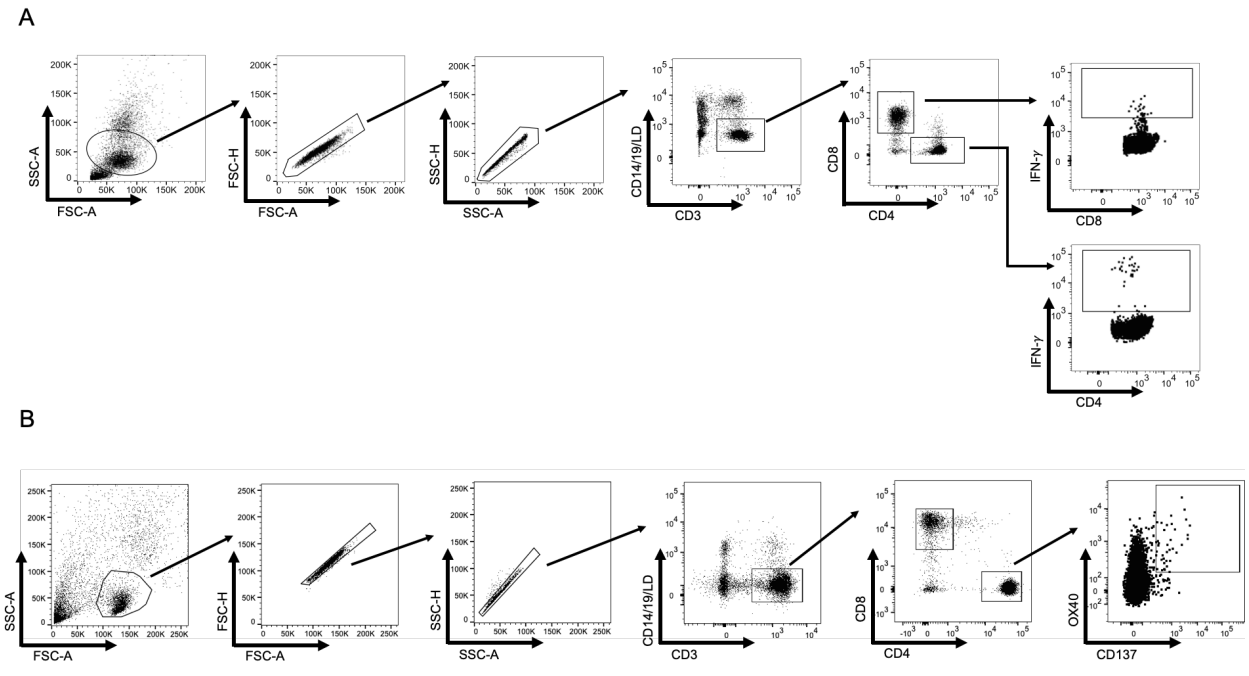

Fig. S5 Gating strategy adopted in IFN-γ Fluorospot and AIM assay: (A) Human PBMCs isolated from HCMV+ subjects were stimulated with each scoring peptide to identify HCMV-specific IFN-γ producing CD4+ and CD8+ T cells. (B) Human PBMCs isolated from HCMV+ and HCMV- subjects were stimulated with each megapool generated to identify HCMV-specific activation-induced marker assay positive (OX40+ CD137+) CD4+ T cells.

783 **Table 1: Details of HCMV specific 235 epitopes identified in the screen.**

S. No	Peptide sequence	Peptide length	ORF(s)	No. of subjects responding	Magnitude of response
1	NGIRWQYQELQYLVE	15	ORFL46W, ORFL46W.iORF1_(UL13), ORFL46W.iORF2	2	222
2	RYNALTVRSRDSLLL	15	ORFL46W, ORFL46W.iORF1_(UL13), ORFL46W.iORF2	2	204
3	RVRTWFVQRTTLWRR	15	ORFL46W, ORFL46W.iORF1_(UL13), ORFL46W.iORF2	1	60
4	GLWVSSYLVRRPMTI	15	ORFL46W, ORFL46W.iORF1_(UL13), ORFL46W.iORF2	2	890
5	QGATYQLSIVRQAMQ	15	ORFL46W.iORF1_(UL13)	1	650
6	GAGLRQLRQQLTVRW	15	ORFL46W.iORF2	1	20
7	MRTVPVTKLYTSRMV	15	ORFL49W_(UL16)(UL16P?)	1	5677
8	AITLFFFLLALRIPQ	15	ORFL49W.iORF1	1	207
9	ALFTHFVGRPRHCRL	15	ORFL50W_(UL17)	1	57
10	MLGIRAMLVMLDYYW	15	ORFL53W_(UL20)	1	350
11	PSVRMDFRARRPLRR	15	ORFL55C_(UL21A)	3	1740
12	ARRLWILSLLAVTLT	15	ORFL57W_(UL22A), ORFL57W.iORF1	1	100
13	LLAVTLTVALAAPSQ	15	ORFL57W_(UL22A)	2	6420
14	KDRCLVIRRRWRLVR	15	ORFL64C_(UL23)	1	60

15	FVAESITEFLNIGLR	15	ORFL64C_(UL23)	1	530
16	HENGIYYGTRSMRKL	15	ORFL64C_(UL23), ORFL64C.iORF1	1	827
17	FCRRFFFPDRPDFFL	15	ORFL65C	1	107
18	AEDSVFTSTRARSAT	15	ORFL70W_(UL25)	1	490
19	KFVLQDFDVQHLRRL	15	ORFL70W_(UL25)	1	40
20	IINYYYVAQKKARHM	15	ORFL70W_(UL25)	1	163
21	ALALHFLTSRKGVTD	15	ORFL70W_(UL25)	1	40
22	LMITHFQRTIRVLRC	15	ORFL70W_(UL25)	3	2421
23	DFLRVVRQQDAFICT	15	ORFL70W_(UL25)	2	174
24	ICVARLQAQPSSRHI	15	ORFL70W_(UL25)	1	37
25	GVSSVTLLKIFSQVP	15	ORFL70W_(UL25)	2	220
26	VLATLAAVRTRRRSV	15	ORFL71C, ORFL71C.iORF1 (UL24)	2	340
27	EAYVRINAGQVLPVV	15	ORFL71C, ORFL71C.iORF1 (UL24)	1	1853
28	LHCMRYLTSSLVKRY	15	ORFL71C	1	150
29	KRYFRPLLRAWSLGL	15	ORFL71C, ORFL71C.iORF1 (UL24)	4	1388
30	HLLRNIKTAFGMRVL	15	ORFL71C, ORFL71C.iORF1 (UL24)	2	1093
31	ARNLMEFARVGLRAV	15	ORFL71C.iORF1 (UL24)	1	1450
32	TGLVLLLLLLVVRLL	15	ORFL73C	1	1440
33	MLFRPTISNSIPRCR	15	ORFL76C	1	47
34	LRIIRLLRASIRHEY	15	ORFL79C_(UL27)	1	810
35	RAHIQKFERLHVRRF	15	ORFL79C_(UL27)	1	2523
36	SLQFIGLQRRDVVAL	15	ORFL92C_(UL32)	1	83

37	RDVVALVNFLRHLTQ	15	ORFL92C_(UL32)	1	1710
38	RRTVLFNELMLWLGY	15	ORFL92C_(UL32)	1	180
39	VNAVNKLVYTGRLIM	15	ORFL92C_(UL32)	1	340
40	KELRMCLSFDSNYCR	15	ORFL92C_(UL32)	1	127
41	GMKTVAFDLSSPQKS	15	ORFL92C.iORF1	1	193
42	NAIVLITQLLTNRVL	15	ORFL93W_(UL33)	1	37
43	STNFLTLTVLPFIVL	15	ORFL93W_(UL33)	1	63
44	VLPFIVLSNQWLLPA	15	ORFL93W_(UL33)	1	247
45	FATVALIAADRYRVL	15	ORFL93W_(UL33)	4	2310
46	SYRSTYIILLLTWFA	15	ORFL93W_(UL33)	3	3990
47	LTLRRTIGTLSRLVP	15	ORFL93W_(UL33)	1	163
48	RRRMVSVTLFSPYSV	15	ORFL98W.iORF1, ORFL98W.iORF2	1	53
49	GRLMEVRQRNGRLRR	15	ORFL100C	1	30
50	WPERCFIQLRSRSAL	15	ORFL101C, ORFL101C.iORF1_(UL36)	3	313
51	GPGFMRYQLIVLIGQ	15	ORFL101C, ORFL101C.iORF1_(UL36)	1	3167
52	IQTMELMIRTVPRIT	15	ORFL101C, ORFL101C.iORF1_(UL36)	2	384
53	EFLVRQYVLVDTFGV	15	ORFL101C	2	104
54	RREAIVRLEKTPTCQ	15	ORFL101C, ORFL101C.iORF1_(UL36)	2	407
55	RRRFKVCDVGRRHII	15	ORFL101C, ORFL101C.iORF1_(UL36)	1	63
56	RHRFLWQRRRRARLL	15	ORFL103C_(vMIA), ORFL104C_(UL37)	1	1000

57	GSFSSFYSQIARSLG	15	ORFL105C_(UL40)	1	363
58	FLKKMLLCALKGRAS	15	ORFL115C_(UL45), ORFL115C.iORF1	1	930
59	MPVQRLTVNVARCVF	15	ORFL115C_(UL45)	1	20
60	KFIFELYRLPRLSIA	15	ORFL115C_(UL45)	1	173
61	ASKIKMLETRVTLAL	15	ORFL116W_(UL47)	1	140
62	ATMLSKYTRMSSLFN	15	ORFL127C_(UL48A)	2	650
63	AFKLDLLRMIAVSRT	15	ORFL127C_(UL48A)	2	477
64	MLFFQRYAPAFVTGY	15	ORFL143C_(UL54)	1	57
65	DLKYILTRLEYLYKV	15	ORFL143C_(UL54)	1	30
66	DPSYVREHGVPIHAD	15	ORFL143C_(UL54)	1	123
67	TDLIRFERNIVCTSM	15	ORFL145C_(UL55)	3	273
68	EGIMVVYKRNIVAHT	15	ORFL145C_(UL55)	1	637
69	HTFKVRVYQKVLTFR	15	ORFL145C_(UL55)	1	423
70	YQKVLTFRRSYAYIH	15	ORFL145C_(UL55)	1	40
71	RRSYAYIHTTYLLGS	15	ORFL145C_(UL55)	5	2730
72	QLMPDDYSNTHSTRY	15	ORFL145C_(UL55)	5	45517
73	NLNCMVTITTARSKY	15	ORFL145C_(UL55)	2	4810
74	NADKFFIFPNYTIVS	15	ORFL145C_(UL55)	4	5120
75	GLVVFWQGIKQKSLV	15	ORFL145C_(UL55)	1	53
76	QLQFTYDTLRGYINR	15	ORFL145C_(UL55)	3	2236
77	LRGYINRALAQIAEA	15	ORFL145C_(UL55)	3	30337
78	KELSKINPSAILSAI	15	ORFL145C_(UL55)	3	18557
79	AILSAIYNKPIAARF	15	ORFL145C_(UL55)	5	11264
80	ASCVTINQTSVKVLR	15	ORFL145C_(UL55)	5	8941
81	YLFKRMIDLSSISTV	15	ORFL145C_(UL55)	1	67
82	EQAYQMLLALARLDA	15	ORFL145C_(UL55)	4	21807

83	LLDRLRHRKNGYRHL	15	ORFL145C.iORF1	3	12544
84	QILWTDGLARRTRDR	15	ORFL145C.iORF2	1	37
85	RVGITIQQLNVYHQL	15	ORFL146C_(UL56)	1	963
86	TMRSVFEMQRIRHGA	15	ORFL147C	1	67
87	NIFLVGFYLLVPYLG	15	ORFL147C	1	1633
88	SLLILVVLLLIYRCC	15	ORFL159W	1	23
89	LSYMKYHHLHGLPVN	15	ORFL161C_(UL69)	3	879
90	VELCLGAGAGHVVVV	15	ORFL162W	1	383
91	RSSWRASCVEVPKKP	15	ORFL165W	1	370
92	MQKYFSLDNFLHDYV	15	UL70	2	20343
93	QTIYFLGLTALLLRY	15	ORFL181C_(UL74)	1	583
94	SFYLVNAMSRNLFRV	15	ORFL181C_(UL74)	1	43
95	TMRKLKRKQALVKEQ	15	ORFL181C_(UL74)	1	1563
96	TAVSEFMKNTHVLIR	15	ORFL181C.iORF1	1	747
97	WREDVLMDRVRKRYL	15	ORFL189W_(UL77)	1	67
98	IKMWFLLGAPMIAVL	15	ORFL196W_(UL78), ORFL196W.iORF1	3	2867
99	LFIIAFFSREPTKDL	15	ORFL196W_(UL78)	1	190
100	PKSFTLTRIHPEYIV	15	ORFL202C_(UL82/pp71)	2	340
101	PEYIVQIQNAFETNQ	15	ORFL202C_(UL82/pp71)	4	527
102	GALTLVIPSWHVFAS	15	ORFL202C_(UL82/pp71)	2	190
103	CRSATSLVGNTNADV	15	ORFL203W	1	30
104	SSCAHTTCRSATSLV	15	ORFL203W	2	104
105	SWLGQMLRPVGLCTL	15	ORFL204W	1	43
106	QTGIHVRVSQPSLIL	15	ORFL205C_(UL83/pp65), ORFL205C.iORF1	11	33563
107	MSIYVYALPLKMLNI	15	ORFL205C_(UL83/pp65)	1	83

108	PLKMLNIPSINVHHY	15	ORFL205C_(UL83/pp65)	7	2920
109	ATKMQVIGDQYVKVY	15	ORFL205C_(UL83/pp65), ORFL205C.iORF1	2	4637
110	PKNMIIKPGKISHIM	15	ORFL205C_(UL83/pp65), ORFL205C.iORF1	5	538
111	PGKISHIMLDVAFTS	15	ORFL205C_(UL83/pp65), ORFL205C.iORF1	9	2386
112	MNGQQIFLEVQAIRE	15	ORFL205C_(UL83/pp65), ORFL205C.iORF1	6	3990
113	ELRQYDPVAALFFFD	15	ORFL205C_(UL83/pp65)	8	1106
114	GILARNLVPMVATVQ	15	ORFL205C_(UL83/pp65), ORFL205C.iORF1	11	34633
115	ALFFFDIDLLLQRGP	15	ORFL205C.iORF1	2	73
116	RVTGLVFSVVFSVSL	15	ORFL206W	4	6380
117	LTWCVIADRQPRFSV	15	ORFL206W	3	240
118	RPKRRVVAPFRVAAA	15	ORFL207W	2	283
119	APFRVAAAGETPLGR	15	ORFL207W	6	1089
120	IPQRLHLIKHYQLGL	15	ORFL209C_(UL85)	1	437
121	IVPMPLALEINQRLL	15	ORFL209C_(UL85)	1	283
122	LASELTMTYVRKLAL	15	ORFL209C_(UL85)	1	37
123	HSILADFNSYKAHLT	15	ORFL212C_(UL86) Major Capsid Protein	1	27
124	FHELRTWEIMEHMRL	15	ORFL212C_(UL86) Major Capsid Protein	1	7343
125	PQLLFHYRNLVAVLR	15	ORFL212C_(UL86) Major Capsid Protein	1	60

126	RNLVAVLRLVTRISA	15	ORFL212C_(UL86) Major Capsid Protein	1	20
127	LFLAVQFVGEHVKVL	15	ORFL212C_(UL86) Major Capsid Protein	1	53
128	VRVQDLFRVFPMNVY	15	ORFL212C_(UL86) Major Capsid Protein	1	43
129	LGYNSKFYSPCAQYF	15	ORFL212C_(UL86) Major Capsid Protein	1	20
130	TQEALPILSTTTLAL	15	ORFL212C_(UL86) Major Capsid Protein	1	407
131	PFTVLRLSYAYRIFA	15	ORFL229W_(UL98)	1	33
132	AREFLLSHDAALFRA	15	ORFL229W_(UL98)	1	23
133	MLIQQYVLSQYYIKK	15	ORFL229W_(UL98)	1	20
134	RLGTAATQIQKQTLY	15	ORFL233C	1	30
135	KTQIFNKLFTNRISV	15	ORFL236C	1	1587
136	VRSLAVDAQHAAKRV	15	ORFL238W	1	53
137	LEERDEWVRSLAVDA	15	ORFL238W	1	47
138	AAITVVPVITQSRLA	15	ORFL245C	3	450
139	PWYPITQARTLELTP	15	ORFL246C	2	996
140	MSTKRSTVPWYPITQ	15	ORFL246C	3	477
141	LRVTFHRVKPTLQRE	15	ORFL248W.iORF1	2	830
142	SGRVILWTTLRLCIL	15	ORFL249C	1	20
143	VVRKYWTFTNPNRIL	15	ORFL251W, ORFL252W, ORFL253W_(UL112), ORFL253W.iORF1, ORFL253W.iORF2	3	16876

144	TFDVRQFVFDNARLV	15	ORFL251W, ORFL252W, ORFL253W_(UL112), ORFL253W.iORF1, ORFL253W.iORF2	6	13736
145	VRGGIVFNKSVSSVV	15	ORFL251W, ORFL252W, ORFL253W_(UL112), ORFL253W.iORF1, ORFL253W.iORF2	5	2691
146	GNLQVTYVRHYLKNH	15	ORFL253W_(UL112), ORFL253W.iORF1, ORFL253W.iORF2	4	655
147	AVAFLNYSSSSSAVS	15	ORFL253W_(UL112), ORFL253W.iORF1, ORFL253W.iORF2	3	2151
148	AGLMMMRRMRRAPAE	15	ORFL253W_(UL112)	1	490
149	CDLPLVSSRLLPETS	15	ORFL253W_(UL112)	1	123
150	CEIKPYVVNPVVATA	15	ORFL253W_(UL112)	3	2583
151	DPLLRLSQVAGSGRR	15	ORFL253W_(UL112)	2	2067
152	LPLCSTARLRLAPRR	15	ORFL253W.iORF3	1	467
153	RATGNFRSTSLYAAV	15	ORFL253W.iORF3	3	4220
154	RCCTLRFRRRCRARC	15	ORFL253W.iORF4	2	713
155	MSATRHHRCCTLRFR	15	ORFL253W.iORF4	1	277
156	RVFCLSADWIRFLSL	15	ORFL254C_(UL114)	2	846
157	HLGWQTLSNHVIRRL	15	ORFL254C_(UL114)	1	127
158	TVVRLHVQIAGRSFT	15	ORFL258C_(UL119)	1	213
159	SCTHPYVISLVTPLT	15	ORFL260C_(UL121)	1	80
160	ISLVTPLTINATLRL	15	ORFL260C_(UL121)	1	317

161	CRVDADLGLLYAVCL	15	ORFL260C_(UL121)	1	673
162	VCLILSFSIVTAALW	15	ORFL260C_(UL121)	1	43
163	MFFLAIRDHDTAGGI	15	ORFL261W	1	1637
164	LQTMLRKEVNSQLSL	15	ORFL264C_(UL123) IE1, ORFL265C_(UL122) IE2	2	1606
165	LVKQIKVRVDMVRHR	15	ORFL264C_(UL123) IE1	3	580
166	RVDMVRHRIKEHMLK	15	ORFL264C_(UL123) IE1	2	250
167	LRRKMMYMCYRNIEF	15	ORFL264C_(UL123) IE1	6	1697
168	CSPDEIMSYAQKIFK	15	ORFL264C_(UL123) IE1	2	194
169	EERDKVLTHIDHIFM	15	ORFL264C_(UL123) IE1	2	107
170	VLCCYVLEETSVMLA	15	ORFL264C_(UL123) IE1	1	93
171	ITKPEVISVMKRRIE	15	ORFL264C_(UL123) IE1	1	1600
172	FAQYILGADPLRVCS	15	ORFL264C_(UL123) IE1	1	30
173	EAIVAYTLATAGASS	15	ORFL264C_(UL123) IE1	3	19333
174	TTRPFKVIIKPPVPP	15	ORFL265C_(UL122) IE2	2	424
175	NKGIQIIYTRNHEVK	15	ORFL265C_(UL122) IE2, ORFL265C.iORF1, ORFL265C.iORF2, ORFL265C.iORF3,	7	3794
176	LGSMCNLALSTPFLM	15	ORFL265C_(UL122) IE2, ORFL265C.iORF1, ORFL265C.iORF2	4	668
177	STPFLMEHTMPVTHP	15	ORFL265C_(UL122) IE2, ORFL265C.iORF1, ORFL265C.iORF2, ORFL265C.iORF3,	4	740
178	YRNMIIHAATPVDLL	15	ORFL265C.iORF3	2	130

179	VMVRIFSTNQGGFML	15	ORFL265C.iORF3	2	3560
180	VVVGIVLCLSLASTV	15	ORFL266W_(UL124)	1	1417
181	SPVAAELPHPSPAPM	15	ORFL267C	2	166
182	SYLAVHLRISHRYYH	15	ORFL269C	1	290
183	IAITMVMRFWQYING	15	ORFL270C	3	163
184	TALWLLLGHSRVPRV	15	UL128	1	177
185	AEIRGIVTTMTHSLT	15	ORFL271C_(UL128_truncated)	1	1713
186	NPLYLEADGRIRCGK	15	ORFL271C_(UL128_truncated), UL128	2	884
187	LHRRAAVSGRRSLLQ	15	ORFL271C.iORF1	1	87
188	MLRLLFTLVLLALYG	15	ORFL278C_(UL148)	3	4593
189	HVRLLSYRGDPLVFK	15	ORFL278C_(UL148)	3	333
190	VVRFALYLETLSRIV	15	ORFL278C_(UL148)	2	123
191	FYMNWTLRRSQTHYL	15	ORFL278C_(UL148)	6	16883
192	QVEILKPRGVRHRAI	15	ORFL278C_(UL148)	9	3468
193	FCVYRYNARLTRGYV	15	ORFL278C_(UL148)	3	700
194	TRGYVRYTLSPKARL	15	ORFL278C_(UL148)	7	9337
195	SLDRFIVQYLNTLLI	15	ORFL278C_(UL148)	8	23368
196	PTWSTTVNAHNSFLH	15	ORFL278C.iORF1	1	47
197	DRLSTLAATMCMFDY	15	ORFL279C	1	53
198	LFYRAVALGTLSALV	15	ORFL280C_(UL147A)	3	2633
199	SSIFTSTHRGVIVAP	15	ORFL283W	1	27
200	LSVRYLSLTAYMLLA	15	ORFL284C_(UL147)	1	1200
201	TAYKAFLWKYAKKLN	15	ORFL284C_(UL147)	1	503
202	WKYAKKLNYHYFRLR	15	ORFL284C_(UL147)	1	237
203	VYLWYVRRQLVAFCL	15	ORFL318C_(UL148A)	3	253
204	FPSARDIPKQLPEQP	15	ORFL320W	1	27

205	VVAYVILERLWLAAR	15	ORFL321W.iORF1	1	23
206	IRRWWISVAIVIFIG	15	ORFL321W.iORF2, ORFL321W.iORF3_(UL148D)	3	10480
207	RWQFAVCAASKTATR	15	ORFL322W	1	50
208	PQRLLLTALAIWQRT	15	ORFL324C_(UL150)	1	983
209	PWWRRLRVKRPKFPS	15	ORFS326C, ORFS326C.iORF1_(US1)	1	240
210	LWYLGDYGAILKIYF	15	ORFS337C_(US10)	1	40
211	LFCGACVITRSLLLI	15	ORFS337C_(US10)	1	487
212	MNLVMLILALWAPVA	15	ORFS338C_(US11)	1	553
213	VSEYRVEYSEARCVL	15	ORFS338C_(US11)	1	263
214	MLVVTVFDTTRLFEI	15	ORFS345C_(US17)	1	840
215	VCAFCWLVLPHRLEQ	15	ORFS351C_(US21)	1	1960
216	VSVLYFMPSEPGSAH	15	ORFS351C.iORF2	1	177
217	VFQKTLSMLQGLYLR	15	ORFS352C_(US22)	2	327
218	GLYLRQYDPPALRTY	15	ORFS352C_(US22)	2	633
219	WFLVMREQAAIPQIY	15	ORFS352C_(US22)	4	1100
220	QIYARSLAADYLCCD	15	ORFS352C_(US22)	1	33
221	DFRDLLNFIRQRLCC	15	ORFS352C_(US22)	1	30
222	PSQEILLLCARHLDE	15	ORFS353C_(US23)	3	110
223	TDCWPFEVAPAARLA	15	ORFS353C_(US23)	2	1637
224	LFRAGLMKVYVRRRY	15	ORFS353C_(US23)	1	870
225	VVFMGRFSRVYAYDT	15	ORFS355C_(US24)	1	70
226	EKYMVLVSHNLDELA	15	ORFS355C_(US24)	1	20
227	PRLHCLVTTRSSTRE	15	ORFS355C.iORF1	1	1277
228	LRYKWLIRKDRFIVR	15	ORFS361C_(US26)	1	3247
229	TNIMLQVSNVTNHTL	15	ORFS363W_(US27)	1	58

230	IVVGLPFFLEYAKHH	15	ORFS363W_(US27)	2	1250
231	YNRMVRFIINYVGKW	15	ORFS363W_(US27)	1	23
232	ITFCLYVGQFLAYVR	15	ORFS363W_(US27)	1	27
233	HDPLGLTRFIMRQLM	15	ORFS370W_(US33A)	1	473
234	FIMRQLMMYPLVLPF	15	ORFS370W_(US33A)	1	530
235	GLVYRELHDFYGYLQ	15	ORFS371W_(US34)	1	963

802 **Table 2: Details of HCMV specific class II epitopes from IEDB**

S. No	Peptide sequence	Peptide length	ORF	Antigen Name from IEDB
1	HINSHSQCYSSYSRVIA	17	ORFL145C_(UL55)	glycoprotein B
2	SRVIAGTVFVAYHRD	15	ORFL145C_(UL55)	glycoprotein B
3	CMVTITTARSKYPYH	15	ORFL145C_(UL55)	glycoprotein B
4	VFETTGGLVVFWQGI	15	ORFL145C_(UL55)	glycoprotein B
5	MQLIPDDYSNTHSTRYVTVK	20	ORFL145C_(UL55)	glycoprotein B
6	LPLKMLNIPSINVH	14	ORFL205C_(UL83/pp65)	65 kDa lower matrix phosphoprotein
7	PQYSEHPTFTSQYRIQ	16	ORFL205C_(UL83/pp65)	65 kDa lower matrix phosphoprotein
8	FTSQYRIQGKLEYRHT	16	ORFL205C_(UL83/pp65)	65 kDa lower matrix phosphoprotein
9	PPWQAGILARNLVPMV	16	ORFL205C_(UL83/pp65)	65 kDa lower matrix phosphoprotein
10	KYQEFFWDANDIYRIF	16	ORFL205C_(UL83/pp65)	65 kDa lower matrix phosphoprotein
11	GPISGHVLKAVFSRG	15	ORFL205C_(UL83/pp65)	65 kDa lower matrix phosphoprotein
12	LLQTGIHVRVSQPSL	15	ORFL205C_(UL83/pp65)	65 kDa lower matrix phosphoprotein
13	IYVYALPLKMLNIPS	15	ORFL205C_(UL83/pp65)	65 kDa lower matrix phosphoprotein

14	LPLKMLNIPSINVHH	15	ORFL205C_(UL83/pp65)	65 kDa lower matrix phosphoprotein
15	KDVALRHVVCAHELV	15	ORFL205C_(UL83/pp65)	65 kDa lower matrix phosphoprotein
16	RHVVCAHELVCSMEN	15	ORFL205C_(UL83/pp65)	65 kDa lower matrix phosphoprotein
17	CSMENTRATKMQVIG	15	ORFL205C_(UL83/pp65)	65 kDa lower matrix phosphoprotein
18	TRATKMQVIGDQYVK	15	ORFL205C_(UL83/pp65)	65 kDa lower matrix phosphoprotein
19	MQVIGDQYVKVYLES	15	ORFL205C_(UL83/pp65)	65 kDa lower matrix phosphoprotein
20	VYLESFCEDVPSGKL	15	ORFL205C_(UL83/pp65)	65 kDa lower matrix phosphoprotein
21	FCEDVPSGKLFMHVT	15	ORFL205C_(UL83/pp65)	65 kDa lower matrix phosphoprotein
22	LGSDVEEDLTMTRNP	15	ORFL205C_(UL83/pp65)	65 kDa lower matrix phosphoprotein
23	EEDLTMTRNPQPFMR	15	ORFL205C_(UL83/pp65)	65 kDa lower matrix phosphoprotein
24	QPFMRPHERNGFTVL	15	ORFL205C_(UL83/pp65)	65 kDa lower matrix phosphoprotein
25	KISHIMLDVAFTSHE	15	ORFL205C_(UL83/pp65)	65 kDa lower matrix phosphoprotein
26	MLDVAFTSHEHFGLL	15	ORFL205C_(UL83/pp65)	65 kDa lower matrix phosphoprotein

27	FTSHEHFGLLCPKSI	15	ORFL205C_(UL83/pp65)	65 kDa lower matrix phosphoprotein
28	PQYSEHPTFTSQYRI	15	ORFL205C_(UL83/pp65)	65 kDa lower matrix phosphoprotein
29	SQYRIQGKLEYRHTW	15	ORFL205C_(UL83/pp65)	65 kDa lower matrix phosphoprotein
30	YRHTWDRHDEGAAQG	15	ORFL205C_(UL83/pp65)	65 kDa lower matrix phosphoprotein
31	IHNPAVFTWPPWQAG	15	ORFL205C_(UL83/pp65)	65 kDa lower matrix phosphoprotein
32	PWQAGILARNLVPMV	15	ORFL205C_(UL83/pp65)	65 kDa lower matrix phosphoprotein
33	ATVQGQNLKYQEFFW	15	ORFL205C_(UL83/pp65)	65 kDa lower matrix phosphoprotein
34	QNLKYQEFFWDANDI	15	ORFL205C_(UL83/pp65)	65 kDa lower matrix phosphoprotein
35	QEFFWDANDIYRIFA	15	ORFL205C_(UL83/pp65)	65 kDa lower matrix phosphoprotein
36	ELEGVWQPAAQPKRR	15	ORFL205C_(UL83/pp65)	65 kDa lower matrix phosphoprotein
37	IFLEVQAIRETVELR	15	ORFL205C_(UL83/pp65)	65 kDa lower matrix phosphoprotein
38	PPWQAGILARNLVPM	15	ORFL205C_(UL83/pp65)	65 kDa lower matrix phosphoprotein
39	DVPSGKLFMHVTLGS	15	ORFL205C_(UL83/pp65)	65 kDa lower matrix phosphoprotein

40	KLFMHVTLGSDVEED	15	ORFL205C_(UL83/pp65)	65 kDa lower matrix phosphoprotein
41	DVEEDLTMTRNPQPF	15	ORFL205C_(UL83/pp65)	65 kDa lower matrix phosphoprotein
42	VAFTSHEHFGLLCPK	15	ORFL205C_(UL83/pp65)	65 kDa lower matrix phosphoprotein
43	SEHPTFTSQYRIQGK	15	ORFL205C_(UL83/pp65)	65 kDa lower matrix phosphoprotein
44	LEYRHTWDRHDEGAA	15	ORFL205C_(UL83/pp65)	65 kDa lower matrix phosphoprotein
45	PLKMLNIPSINVHHY	15	ORFL205C_(UL83/pp65)	65 kDa lower matrix phosphoprotein
46	KVYLESFCEDVPSGK	15	ORFL205C_(UL83/pp65)	65 kDa lower matrix phosphoprotein
47	TLGSDVEEDLTMTRN	15	ORFL205C_(UL83/pp65)	65 kDa lower matrix phosphoprotein
48	ASTSAGRKRKSASSA	15	ORFL205C_(UL83/pp65)	65 kDa lower matrix phosphoprotein
49	ACTSGVMTRGRLKAE	15	ORFL205C_(UL83/pp65)	65 kDa lower matrix phosphoprotein
50	AGILARNLVPMVATV	15	ORFL205C_(UL83/pp65)	65 kDa lower matrix phosphoprotein
51	EPDVYYTSAFVFPTK	15	ORFL205C_(UL83/pp65)	65 kDa lower matrix phosphoprotein
52	QVIGDQYVKVYLESF	15	ORFL205C_(UL83/pp65)	65 kDa lower matrix phosphoprotein

53	FFWDANDIYRIFAEL	15	ORFL205C_(UL83/pp65)	65 kDa lower matrix phosphoprotein
54	LVSQYTPDSTPCHRG	15	ORFL205C_(UL83/pp65)	65 kDa lower matrix phosphoprotein
55	SHIMLDVAFTSHEH	14	ORFL205C_(UL83/pp65)	65 kDa lower matrix phosphoprotein
56	DEDSDNEIHNPAVFTW	16	ORFL205C_(UL83/pp65)	65 kDa lower matrix phosphoprotein
57	SQYTPDSTPCHRG	13	ORFL205C_(UL83/pp65)	65 kDa lower matrix phosphoprotein
58	KPGKISHIMLDVA	13	ORFL205C_(UL83/pp65)	65 kDa lower matrix phosphoprotein
59	PTFTSQYRIQGKL	13	ORFL205C_(UL83/pp65)	65 kDa lower matrix phosphoprotein
60	DTPVLPHETRLLQTGIHVRV	20	ORFL205C_(UL83/pp65)	65 kDa lower matrix phosphoprotein
61	INVHHYPSAAERKHRHLPVA	20	ORFL205C_(UL83/pp65)	65 kDa lower matrix phosphoprotein
62	LLQRGPQYSEHPTFT	15	ORFL205C_(UL83/pp65)	65 kDa lower matrix phosphoprotein
63	ALFFFDIDLLLQRGPQYSE	19	ORFL205C_(UL83/pp65)	65 kDa lower matrix phosphoprotein
64	DQYVKVYLESFCEDVPSGKL	20	ORFL205C_(UL83/pp65)	65 kDa lower matrix phosphoprotein
65	MTRNPQPFMRPHERNGFTVL	20	ORFL205C_(UL83/pp65)	65 kDa lower matrix phosphoprotein

66	MISVLGPISGHVLKAVFSRG	20	ORFL205C_(UL83/pp65)	65 kDa lower matrix phosphoprotein
67	ASGKQMWQARLTVSGLAWTR	20	ORFL205C_(UL83/pp65)	65 kDa lower matrix phosphoprotein
68	LPLKMLNIPSINVHHYPSAA	20	ORFL205C_(UL83/pp65)	65 kDa lower matrix phosphoprotein
69	PHETRLLQTGIHVRVSQPSL	20	ORFL205C_(UL83/pp65)	65 kDa lower matrix phosphoprotein
70	IYVYALPLKMLNIPSINVHH	20	ORFL205C_(UL83/pp65)	65 kDa lower matrix phosphoprotein
71	QYDPVAALFFFDIDLLLQRG	20	ORFL205C_(UL83/pp65)	65 kDa lower matrix phosphoprotein
72	RQYDPVAALFFFDIDL	16	ORFL205C_(UL83/pp65)	65 kDa lower matrix phosphoprotein
73	HETRLLQTGIHVRVS	15	ORFL205C_(UL83/pp65)	65 kDa lower matrix phosphoprotein
74	VYALPLKMLNIPSIN	15	ORFL205C_(UL83/pp65)	65 kDa lower matrix phosphoprotein
75	VALRHVVCAHELVCS	15	ORFL205C_(UL83/pp65)	65 kDa lower matrix phosphoprotein
76	HIMLDVAFTSHEHFG	15	ORFL205C_(UL83/pp65)	65 kDa lower matrix phosphoprotein
77	FTSQYRIQGKLEYRH	15	ORFL205C_(UL83/pp65)	65 kDa lower matrix phosphoprotein
78	YRIQGKLEYRHTWDR	15	ORFL205C_(UL83/pp65)	65 kDa lower matrix phosphoprotein

79	ARNLVPMVATVQGQN	15	ORFL205C_(UL83/pp65)	65 kDa lower matrix phosphoprotein
80	ANDIYRIFAELEGVW	15	ORFL205C_(UL83/pp65)	65 kDa lower matrix phosphoprotein
81	TRQQNQWKEPDVYYT	15	ORFL205C_(UL83/pp65)	65 kDa lower matrix phosphoprotein
82	TERKTPRVTGGGAMA	15	ORFL205C_(UL83/pp65)	65 kDa lower matrix phosphoprotein
83	NLKYQEFFWDANDIY	15	ORFL205C_(UL83/pp65)	65 kDa lower matrix phosphoprotein
84	TPRVTGGGAMAGAST	15	ORFL205C_(UL83/pp65)	65 kDa lower matrix phosphoprotein
85	DQYVKVYLESFCEDV	15	ORFL205C_(UL83/pp65)	HCMVUL83
86	GKISHIMLDVAFTSH	15	ORFL205C_(UL83/pp65)	HCMVUL83
87	EHPTFTSQYRIQGKL	15	ORFL205C_(UL83/pp65)	HCMVUL83
88	GQNLKYQEFFWDAND	15	ORFL205C_(UL83/pp65)	HCMVUL83
89	KYQEFFWDANDIYRI	15	ORFL205C_(UL83/pp65)	HCMVUL83
90	IIKPGKISHIMLDVA	15	ORFL205C_(UL83/pp65)	HCMVUL83
91	TRATKMQVIGDQYVKVYLES	20	ORFL205C_(UL83/pp65)	HCMVUL83
92	KLFMHVTLGSDVEEDLTMTR	20	ORFL205C_(UL83/pp65)	HCMVUL83
93	KPGKISHIMLDVAFTSHEHF	20	ORFL205C_(UL83/pp65)	HCMVUL83
94	LPVADAVIHASGKQMWQARL	20	ORFL205C_(UL83/pp65)	HCMVUL83
95	GSDSDEELVTTERKTPRVTG	20	ORFL205C_(UL83/pp65)	HCMVUL83
96	RHRQDALPGPCIASTPKKHR	20	ORFL205C_(UL83/pp65)	HCMVUL83
97	YQEFFWDANDIYR	13	ORFL205C_(UL83/pp65)	HCMVUL83
98	LAWTRQQNQWKEPDV	15	ORFL205C_(UL83/pp65)	HCMVUL83
99	YQEFFWDANDIYRIF	15	ORFL205C_(UL83/pp65)	HCMVUL83

100	EFFWDANDIYRIF	13	ORFL205C_(UL83/pp65)	HCMVUL83
101	VEEDLTMTRNPQPFM	15	ORFL205C_(UL83/pp65)	HCMVUL83
102	KPGKISHIMLDVAFTSH	17	ORFL205C_(UL83/pp65)	HCMVUL83
103	TSQYRIQGKLEYRHT	15	ORFL205C_(UL83/pp65)	HCMVUL83
104	MSIYVYALPLKMLNI	15	ORFL205C_(UL83/pp65)	HCMVUL83
105	VYYTSAFVFPTKDVA	15	ORFL205C_(UL83/pp65)	HCMVUL83
106	LRQYDPVAALFFFDI	15	ORFL205C_(UL83/pp65)	HCMVUL83
107	GPQYSEHPTFTSQYRI	16	ORFL205C_(UL83/pp65)	HCMVUL83
108	HPTFTSQYRIQGKLE	15	ORFL205C_(UL83/pp65)	HCMVUL83
109	TRLLQTGIHVRVSQP	15	ORFL205C_(UL83/pp65)	HCMVUL83
110	RNGFTVLCPKNMIIK	15	ORFL205C_(UL83/pp65)	HCMVUL83
111	PISGHVLKAVFSRGD	15	ORFL205C_(UL83/pp65)	HCMVUL83
112	GIHVRVSQPSLILVS	15	ORFL205C_(UL83/pp65)	HCMVUL83
113	IHASGKQMWQARLTV	15	ORFL205C_(UL83/pp65)	HCMVUL83
114	GKQMWQARLTVSGLA	15	ORFL205C_(UL83/pp65)	HCMVUL83
115	ENTRATKMQVIGDQY	15	ORFL205C_(UL83/pp65)	HCMVUL83
116	ATKMQVIGDQYVKVY	15	ORFL205C_(UL83/pp65)	HCMVUL83
117	RPHERNGFTVLCPKN	15	ORFL205C_(UL83/pp65)	HCMVUL83
118	AQGDDDVWTSGSDSD	15	ORFL205C_(UL83/pp65)	HCMVUL83
119	SSATACTSGVMTRGR	15	ORFL205C_(UL83/pp65)	HCMVUL83
120	YRIFAELEGVWQPAA	15	ORFL205C_(UL83/pp65)	HCMVUL83
121	AELEGVWQPAAQPKR	15	ORFL205C_(UL83/pp65)	HCMVUL83
122	AVFSRGDTPVLPHET	15	ORFL205C_(UL83/pp65)	phosphorylated matrix protein (pp65)
123	ALPLKMLNIPSINVH	15	ORFL205C_(UL83/pp65)	pp65
124	HVLKAVFSRGDTPVL	15	ORFL205C_(UL83/pp65)	pp65
125	AHELVCSMENTRATKMQVIG	20	ORFL205C_(UL83/pp65)	tegument protein pp65

126	FCEDVPSGKLFMHVTLGSDV	20	ORFL205C_(UL83/pp65)	tegument protein pp65
127	TLGSDVEEDLTMTRNPQPF	19	ORFL205C_(UL83/pp65)	tegument protein pp65
128	LLQTGIHVRVSQPSLILV	18	ORFL205C_(UL83/pp65)	tegument protein pp65
129	SICPSQEPMSIYVYA	15	ORFL205C_(UL83/pp65)	tegument protein pp65
130	SQEPMSIYVYALPLK	15	ORFL205C_(UL83/pp65)	tegument protein pp65
131	LNIPSINVHHYPSAA	15	ORFL205C_(UL83/pp65)	tegument protein pp65
132	HDVSKGDDNKLGGALQAKA	19	ORFL264C_(UL123) IE1	55 kDa immediate-early protein 1
133	ALQAKARDKKDELRRKMMY	19	ORFL264C_(UL123) IE1	55 kDa immediate-early protein 1
134	KEHMLKKYTQTEEKF	15	ORFL264C_(UL123) IE1	55 kDa immediate-early protein 1
135	QTEEKFTGAFNMMGGCLQN	19	ORFL264C_(UL123) IE1	55 kDa immediate-early protein 1
136	MGGCLQNALDILDKVHEPFE	20	ORFL264C_(UL123) IE1	55 kDa immediate-early protein 1
137	AIVAYTLATAGVSSSDSLV	19	ORFL264C_(UL123) IE1	55 kDa immediate-early protein 1
138	TMQSMYENYIVPEDKREMW	19	ORFL264C_(UL123) IE1	55 kDa immediate-early protein 1
139	RRKMMYMCYRNIEFFTKNS	19	ORFL264C_(UL123) IE1	55 kDa immediate-early protein 1
140	FFTKNSAFPKTTNGCSQAM	19	ORFL264C_(UL123) IE1	55 kDa immediate-early protein 1
141	CVETMCNEYKVTSDACMMT	19	ORFL264C_(UL123) IE1	55 kDa immediate-early protein 1

142	DACMMTMYGGASLLSEFCR	19	ORFL264C_(UL123) IE1	55 kDa immediate-early protein 1
143	NYIVPEDKREMWMACIKELH	20	ORFL264C_(UL123) IE1	55 kDa immediate-early protein 1
144	VRHRIKEHMLKKYTQTEEKF	20	ORFL264C_(UL123) IE1	55 kDa immediate-early protein 1
145	VRVDMVRHRIKEHML	15	ORFL264C_(UL123) IE1	55 kDa immediate-early protein 1
146	VKQIKVRVDMVRHRI	15	ORFL264C_(UL123) IE1	55 kDa immediate-early protein 1
147	VRHRIKEHMLKKYTQ	15	ORFL264C_(UL123) IE1	55 kDa immediate-early protein 1
148	EQSDEEEEEGAQEER	15	ORFL264C_(UL123) IE1	55 kDa immediate-early protein 1
149	VKSEPVSEIEEVAPE	15	ORFL264C_(UL123) IE1	55 kDa immediate-early protein 1
150	PVSEIEEVAPEEEED	15	ORFL264C_(UL123) IE1	55 kDa immediate-early protein 1
151	LQNALDILDKVHEPF	15	ORFL264C_(UL123) IE1	55 kDa immediate-early protein 1
152	EDKREMWMACIKELH	15	ORFL264C_(UL123) IE1	55 kDa immediate-early protein 1
153	THIDHIFMDILTTCV	15	ORFL264C_(UL123) IE1	55 kDa immediate-early protein 1
154	VLEETSVMLAKRPLI	15	ORFL264C_(UL123) IE1	55 kDa immediate-early protein 1

155	TKPEVISVMKRRIEE	15	ORFL264C_(UL123) IE1	55 kDa immediate-early protein 1
156	RRIEEICMKVFAQYI	15	ORFL264C_(UL123) IE1	55 kDa immediate-early protein 1
157	NIEFFTKNSAFPKTT	15	ORFL264C_(UL123) IE1	regulatory protein IE1
158	LTHIDHIFMDILTTCVETM	19	ORFL264C_(UL123) IE1	regulatory protein IE1
159	AIVAYTLATAGASSSDSLV	19	ORFL264C_(UL123) IE1	UL123; IE1
160	VRVDMVRHRIKEHMLKKYTQ	20	ORFL264C_(UL123) IE1	UL123; IE1
161	DKREMWMACIKELH	14	ORFL264C_(UL123) IE1	UL123; IE1
162	QSMYENYIVPEDKREMWMAC	20	ORFL264C_(UL123) IE1	UL123; IE1
163	TRRGRVKIDEVSRMF	15	ORFL265C_(UL122) IE2	45 kDa immediate-early protein 2
164	GDILAQAVNHAGIDS	15	ORFL265C_(UL122) IE2	45 kDa immediate-early protein 2
165	KTTRPFKVIIKPPVP	15	ORFL265C_(UL122) IE2	45 kDa immediate-early protein 2
166	FKVIIKPPVPPAPIM	15	ORFL265C_(UL122) IE2	45 kDa immediate-early protein 2
167	PEPDFTIQYRNKIID	15	ORFL265C_(UL122) IE2	45 kDa immediate-early protein 2
168	PFTIPSMHQVLDEAI	15	ORFL265C_(UL122) IE2	45 kDa immediate-early protein 2
169	LMQKFPKQVMVRIFS	15	ORFL265C_(UL122) IE2	45 kDa immediate-early protein 2
170	VRIFSTNQGGFMLPI	15	ORFL265C_(UL122) IE2	45 kDa immediate-early protein 2

171	PEDLDTLSLAIEAAI	15	ORFL265C_(UL122) IE2	45 kDa immediate-early protein 2
172	TLSLAIEAAIQDLRN	15	ORFL265C_(UL122) IE2	45 kDa immediate-early protein 2
173	SMHQVLDEAIKACKT	15	ORFL265C_(UL122) IE2	45 kDa immediate-early protein 2
174	KGIQIIYTRNHEVKS	15	ORFL265C_(UL122) IE2	45 kDa immediate-early protein 2
175	ALSTPFLMEHTMPVT	15	ORFL265C_(UL122) IE2	45 kDa immediate-early protein 2
176	FLMEHTMPVTHPPEV	15	ORFL265C_(UL122) IE2	45 kDa immediate-early protein 2
177	PYAVAFQPLLAYAY	14	UL57	single-stranded DNA-binding protein
178	KTQLNRHSYLKDSDFLDAA	19	UL75	envelope glycoprotein H
179	RQTEKHELLVLVKKAQLNRH	20	UL75	Glycoprotein H precursor
180	LDPHAFHLLLNTYGRPIR	18	UL75	Glycoprotein H precursor
181	KAQLNRHSYLKDSDFLDAA	19	UL75	Glycoprotein H precursor
182	DVLKSGRCQMLDRRTVEMA	19	UL75	Glycoprotein H precursor
183	LDKAFHLLLNTYGRPIR	17	UL75	Glycoprotein H precursor
184	KDQLNRHSYLKDPDFLDAA	19	UL75	Glycoprotein H precursor
185	SYLKDSDFLDAAL	13	UL75	HCMVUL75
186	RRIPHFYRVRREVPRTVNE	19	UL86	Major capsid protein
187	MDVNYFKIPNNPRGRASCM	19	UL86	Major capsid protein

803

804

805

Table 3: Demographic characteristics of HCMV (+/-) subjects analyzed in screening and validation studies.

Characteristics	*Screening cohort*	*Validation cohort*	
	HCMV+	**HCMV+**	**HCMV-**
Total participants enrolled, n	19	10	10
Males/females	10/9	3/7	3/7
Median age (range)	65 (28-80)	35.5 (22-55)	28.5 (19-42)
Caucasian, % (n)	68 (13)	40 (4)	40 (4)
Asian, % (n)	16 (3)	10 (1)	20 (2)
African American, % (n)	5 (1)	10 (1)	10 (1)
More than one race, % (n)	0 (0)	30 (3)	30 (3)
Unknown, % (n)	10 (2)	10 (1)	0 (0)